Chem Soc Rev

REVIEW ARTICLE

View Article Online
View Journal | View Issue



Cite this: *Chem. Soc. Rev.*, 2025, **54**, 4502

# Protein-derived cofactors: chemical innovations expanding enzyme catalysis

Angelica Graciano and Aimin Liu *

Protein-derived cofactors, formed through posttranslational modification of a single amino acid or covalent crosslinking of amino acid side chains, represent a rapidly expanding class of catalytic moieties that redefine enzyme functionality. Once considered rare, these cofactors are recognized across all domains of life, with their repertoire growing from 17 to 38 types in two decades in our survey. Their biosynthesis proceeds *via* diverse pathways, including oxidation, metal-assisted rearrangements, and enzymatic modifications, yielding intricate motifs that underpin distinctive catalytic strategies. These cofactors span paramagnetic and non-radical states, including both mono-radical and crosslinked radical forms, sometimes accompanied by additional modifications. While their discovery has accelerated, mechanistic understanding lags, as conventional mutagenesis disrupts cofactor assembly. Emerging approaches, such as site-specific incorporation of non-canonical amino acids, now enable precise interrogation of cofactor biogenesis and function, offering a viable and increasingly rigorous means to gain mechanistic insights. Beyond redox chemistry and electron transfer, these cofactors confer enzymes with expanded functionalities. Recent studies have unveiled new paradigms, such as long-range remote catalysis and redox-regulated crosslinks as molecular switches. Advances in structural biology, mass spectrometry, and biophysical spectroscopy continue to elucidate their mechanisms. Moreover, synthetic biology and biomimetic chemistry are increasingly leveraging these natural designs to engineer enzyme-inspired catalysts. This review integrates recent advances in cofactor biogenesis, reactivity, metabolic regulation, and synthetic applications, highlighting the expanding chemical landscape and growing diversity of protein-derived cofactors and their far-reaching implications for enzymology, biocatalysis, and biotechnology.

Received 3rd February 2025

DOI: 10.1039/d4cs00981a

rsc.li/chem-soc-rev

*Department of Chemistry, The University of Texas at San Antonio, Texas 78249, USA. E-mail: Feradical@utsa.edu*

**Angelica Graciano**

*Angelica Graciano is currently a Chemistry PhD student at the University of Texas at San Antonio (UTSA) under the supervision of Dr Aimin Liu. She obtained her BSc in Biochemistry at UTSA where her undergraduate research helped develop a deep interest in metalloenzymology. Her current research focuses on the elucidation of protein-derived cofactor biogenesis mechanisms through the incorporation of non-canonical amino acids, and characterization of metalloenzymes with functional roles in oxygen activation, amino acid metabolism, and carbohydrate metabolism.*

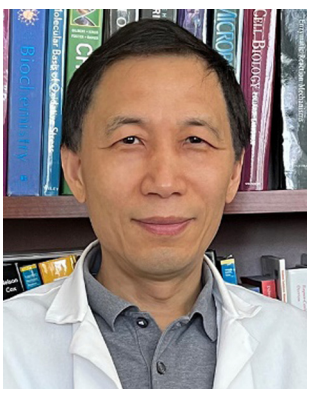

**Aimin Liu**

*Dr Aimin Liu specializes in amino acid chemistry, including metabolism and crosslinking. His research explores redox chemistries mediated by metalloproteins and free radicals, with conceptual contributions like biological charge resonance. He earned his PhD from Stockholm University after a BS from USTC. He held Royal Society scholarships and began his independent career in 2002 and is currently an endowed distinguished Professor of Chemistry and the Lutcher Brown Distinguished Chair in Biochemistry, and a member of the Academy of Distinguished Researchers at the University of Texas at San Antonio. He is an AAAS Fellow (Chemistry) and FRSC.*

# 1. Introduction

Enzymes, the workhorses of biological systems, rely on diverse strategies to catalyze an extraordinary range of chemical reactions. While genetically encoded amino acids provide the fundamental building blocks of proteins, nature often employs additional chemical entities known as cofactors to expand the catalytic repertoire of enzymes. These cofactors—comprising metal ions, exogenous organic molecules (such as vitamins and nucleotides), or complex structures of both endogenous and exogenous origins—reshape the catalytic machinery and modulate catalysis and reaction outcomes. Protein-derived cofactors are frequently encountered in oxidase, oxygenase, reductase, dehydrogenase, carboxylase, catalase, decarboxylase, lyases, hydratases, phosphotriesterase, racemase, sulfatase, synthetase *etc.* They are crucial for a vast array of biological processes, from challenging chemical transformations under mild conditions, metabolism for energy production, and biosynthesis to signal transduction and DNA replication. Typically, these cofactors bind non-covalently to proteins, forming functional holoenzymes.

A fascinating class of cofactors is those ''homemade cofactors''[1] or ''built-in cofactors''[2] generated directly within proteins through covalent unidirectional posttranslational modifications (PTMs) of their constituent amino acid residues (Fig. 1). Among these PTMs, covalent crosslinking of amino acid side chains represents a remarkable strategy for creating specialized protein-derived cofactors. This intramolecular crosslinking, occurring within a single polypeptide chain, results in the formation of new covalent bonds (C–C, C–N, C–O, or C–S) that endow the protein with unique structural and chemical properties. This process is distinct from intermolecular crosslinking, which involves the formation of bonds between separate protein molecules and is often associated with protein aggregation or structural networks. This review focuses specifically on cofactors generated by intramolecular covalent crosslinking, excluding instances of intermolecular crosslinking.

Formally known as protein-derived cofactors, these ''homemade'' intricate, atypical protein structural components are formed by chemical modification of a single amino acid side chain or by crosslinked side chains as a result of PTMs either through direct oxidation by metal/$O_2$- or $H_2O_2$-derived intermediates or through outer sphere oxidation by highly oxidizing exogenous cofactors or auxiliary enzymes.[3,4] These protein-derived cofactors often present significant challenges for prediction. Even advanced artificial intelligence (AI)-powered computational methods, such as the latest iterations of AlphaFold,[5,6] currently lack the accuracy and reliability to consistently identify or predict these cofactors.[5,7–10] Consequently, high-resolution structural studies, such as X-ray crystallography and cryo-electron microscopy (cryo-EM), remain essential for elucidating their precise structures and bonding arrangements. AlphaFold-guided molecular replacement for solving challenging crystal structures is evolving.[11] Complementing these techniques, crosslinked peptide fragmentation (CLPF) mass spectrometry provides a powerful approach for identifying and validating the presence of novel crosslinks in proteins.[12–16] Recent technological advances in rapid data collection at cryogenic temperatures to $^{13}$C-NMR investigations of $^{13}$C-labeled proteins and chemical modification protocols that can be integrated with both UV-visible and fluorescence spectroscopy offer crucial complementary information.[17] These advances have facilitated the discovery of novel protein-derived cofactors. Emerging technologies, such as non-canonical natural and unnatural amino acid substitutions through genetic code expansion, have enabled precise interrogation of cofactor biogenesis and function. The resulting chemical and structural insights are vital for understanding the mechanisms underlying their biosynthesis and the precise role of these cofactors.

Approximately two decades ago, Okeley and van der Donk provided a foundational overview of protein-derived cofactors, identifying 17 distinct types and categorizing them based on their structural complexity.[18] Since then, the field has witnessed significant growth, with the discovery and characterization of numerous new examples. Our current survey expands this list to 38 distinct types (Fig. 1), highlighting the rapid progress in this area. As emphasized in the work of Walsh and others, forming these crosslinked structures can significantly enhance a protein's structural variability by several orders of magnitude, enabling versatile functionalities in biological systems.[4,18–24] This review builds upon the previous seminal work,[18] focusing on protein-derived cofactors that have been characterized structurally and functionally within the past two decades. We will examine cofactors formed autocatalytically or enzymatically by other processing proteins, exploring how these modifications enhance existing protein functions, or add entirely new ones (Fig. 2).

This review is organized as follows: First, we will discuss the various types of covalent crosslinks observed in protein-derived cofactors, categorized by the chemical nature of the bond formed and number of amino acid residues involved. While classifying these cofactors based on the type of bond formed during PTMs might seem intuitive, the frequent occurrence of multiple bond types within a single cofactor makes this approach less practical. Therefore, we maintain a classification based on the number of residues involved in the cofactor structure. Next, we will delve into the biosynthetic pathways leading to their formation, highlighting the enzymes and mechanisms involved. Subsequently, we will explore the diverse functional roles of these cofactors in biological systems, focusing on enzymatic catalysis and other key biological processes. Finally, we will briefly discuss emerging synthetic approaches to mimic these cofactors and their potential applications.

# 2. Protein cofactors derived from posttranslational modifications of single amino acids

A large subclass of protein-derived cofactors arises from PTMs of single amino acid residues within the polypeptide chain,

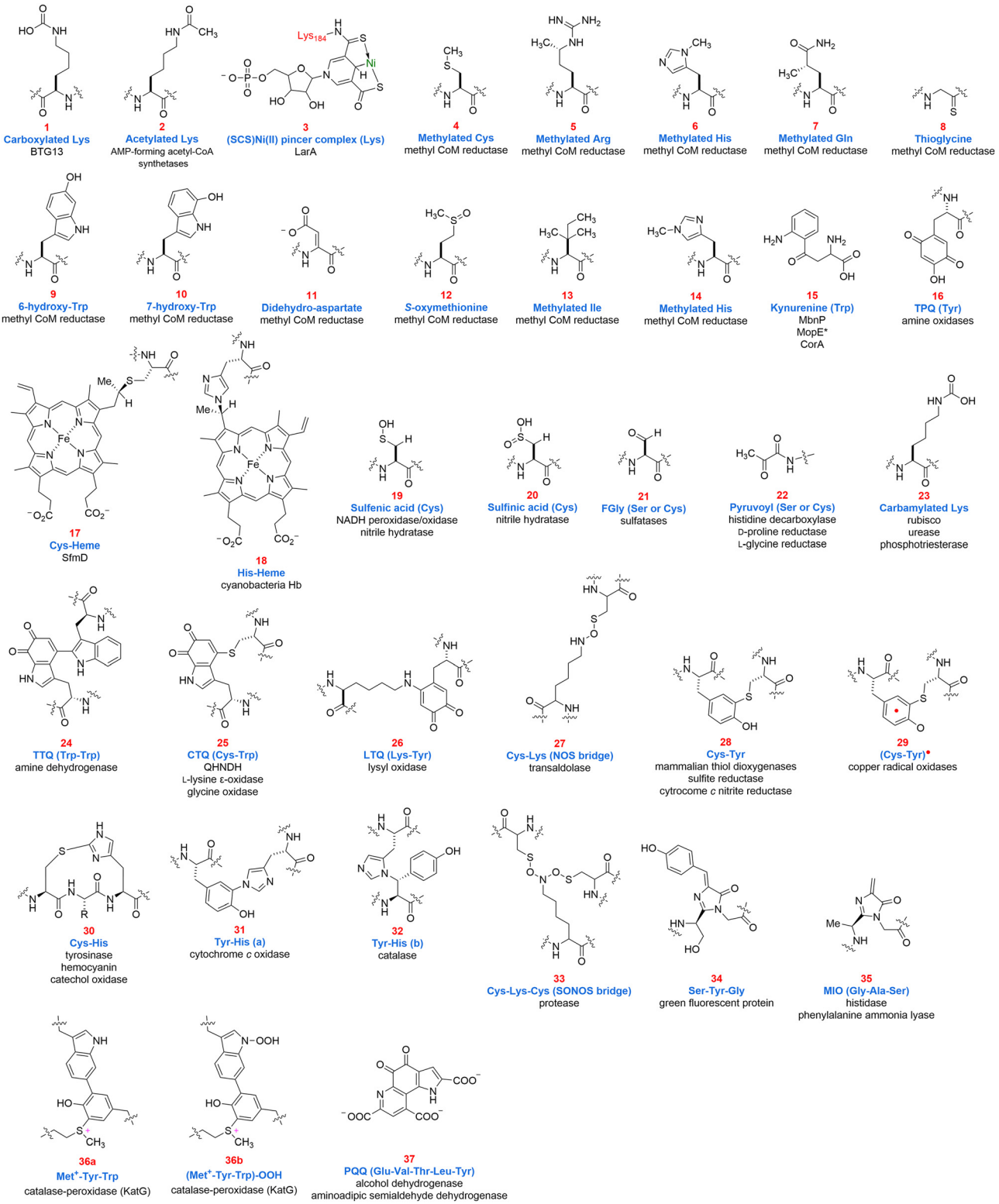


Fig. 1 Thirty-eight structures of identified protein-derived cofactors and their corresponding systems from a total of 38 protein-derived cofactors. Throughout the text, these structures will be referenced by their assigned number. *The straight arrow in **3** indicates coordination.

totaling fifteen, as shown in Table 1. These modifications, encompassing a range of chemical transformations such as oxidation, reduction, carboxylation, and the formation of protein-derived unusual amino acids, generate unique structural motifs that play critical roles in modulating protein functions. Twelve genetically encoded amino acid

 

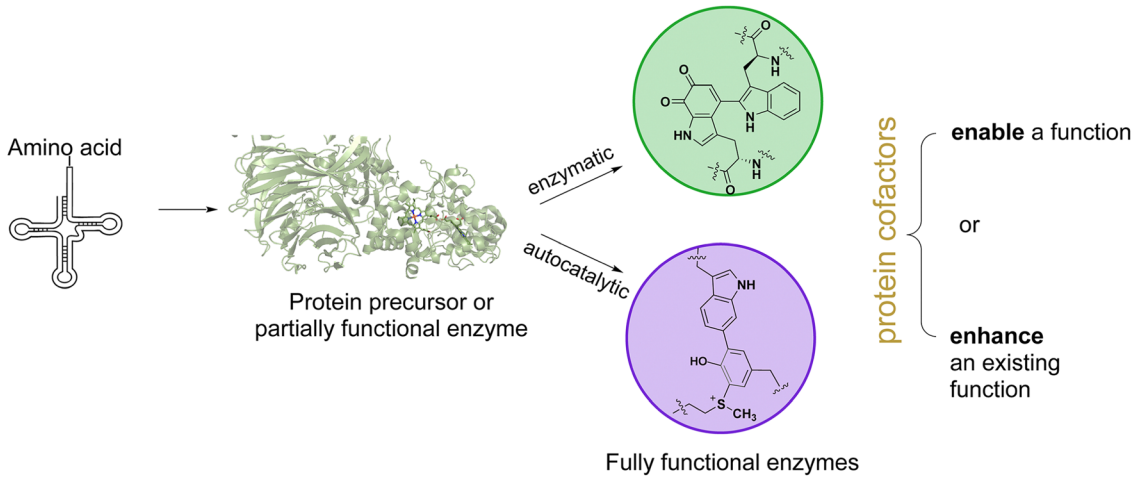


Fig. 2 Overview of the paths that generate posttranslationally modified amino acids. Protein-derived cofactors are either enzymatically or autocatalytically formed and serve to enable a function or enhance an existing function.

residues—Asp, Arg, Cys, Gly, Gln, His, Ile, Lys, Met, Ser, Trp, and Tyr—have been identified as precursors to these modified cofactors (Table 1), highlighting the versatility of the proteinogenic amino acids. This section will explore these single amino acid-derived diverse cofactors, emphasizing their structural diversity, functional significance, and the biochemical pathways leading to their formation. We will divide this section into two subsections based on the final oxidation state of the final cofactor.

### 2.1. Modified single amino acid cofactors

This subsection focuses on single amino acid residues that undergo PTMs to form non-radical cofactors. Several examples illustrate the diverse chemical transformations involved.

**2.1.1. Carboxylated lysine.** During the characterization of the beticolin 1 biosynthetic pathway, a novel non-heme iron-dependent oxygenase, BTG13, was recently identified as the catalyst for anthraquinone ring cleavage.[45] Structural analysis of wild-type BTG13 (Fig. 3A) reveals an unprecedented iron coordination environment comprising four histidines and a carboxylated lysine (Kcx) residue at position 377 (Fig. 1, **1**), which is hydrogen-bonded to His58 and Thr299.[45,63] This Kcx377 acts as a crucial protein-derived cofactor in the oxygenase. Substitution of Lys377 with tyrosine or arginine leads to a complete loss of catalytic activity in BTG13, demonstrating the essential role of Kcx377 in catalysis. Further structural characterization of the H58F and T299V variants reveals a perturbed Kcx377 conformation in H58F and the absence of Kcx377 in T299V, strongly implicating His58 and Thr299 in Kcx377 biogenesis.[45] While the precise mechanism of Kcx377 formation remains to be fully elucidated, these findings underscore the critical roles of His58 and Thr299 in regulating the process of Lys377 carboxylation and, consequently, enzyme reactivity.

Mechanistic investigations into the $C_{4a}$–$C_{10}$ bond cleavage of anthraquinone catalyzed by BTG13, supported by computational studies, propose a stepwise mechanism initiated by hydrogen atom abstraction from $C_{10}$ of the substrate by a ferric superoxide species, Fe(III)–$O_2^{\bullet-}$, generating a substrate radical–Fe(III)–OOH intermediate.[63] Subsequent homolytic O–O bond cleavage and rebound of the distal oxygen to the substrate radical forms a high-valent Fe(IV)=O species. Computational studies further suggest that Kcx377 facilitates the initial electron transfer from the iron center to dioxygen, promoting the formation of Fe(III)–$O_2^{\bullet-}$, the catalytically relevant species.[63]

**2.1.2. Lysine acetylation regulates enzyme activity.** Lysine acetylation (Fig. 1, **2**) is widespread across all domains of life.[64,65] Although it is generally understood that lysine acetylation regulates AMP-forming acetyl-CoA synthetase (AcsA) in bacteria and eukaryotes, the mechanism of action is yet to be elucidated. In AcsA of *Bacillus subtilis*, the acetylation of Lys549 regulates its activity.[66] This lysine residue is conserved in AcsA in bacteria and eukaryotes, suggesting that regulation of enzyme activity through lysine acetylation is evolutionarily conserved.[49]

A recently characterized protein, AcuA, functions as an acetyltransferase, transferring an acetyl group from either acetyl-CoA or acetyl phosphate to Lys549 on AcsA, thereby inactivating this synthetase.[49] Interestingly, this process is reversible, and AcsA activity can be restored through the enzymatic deacetylation of Lys549.[49] The presence of genetically encoded regulatory mechanisms—namely, an acetyltransferase and its corresponding deacetylase—highlights the critical need for AcsA regulation. Given the conservation of this lysine residue, it is speculated that other acetyl-CoA synthetases might regulate their activity similarly, based on metabolic conditions. These findings enhance our understanding of the AMP-forming acetyl-CoA synthetase in cellular metabolism and present potential therapeutic targets for interventions.

**2.1.3. First pincer complex identified in nature.** Pincer ligands are well-established in synthetic organometallic chemistry, prized for their robust coordination properties and ability to stabilize a wide range of metal oxidation states. However,

Table 1 Protein cofactors derived from posttranslational modifications of single amino acids

| Source | Cofactor | New chemical bonds formed | Representative enzyme | Biogenesis | Function | Ref. |
|---|---|---|---|---|---|---|
| Arg | Methylated | C–C | Methyl-coenzyme M reductase | Enzymatic RCMT | Subunit interaction | 25 and 26 |
| Asp | Didehydroaspartate | C=C | Methyl-coenzyme M reductase | TBD | Tune enzyme structure | 27 |
| Cys | Pyruvoyl group | C=O | D-Proline reductase | Autocatalytic | Catalysis | 28 |
| | Pyruvoyl group | C=O | L-Glycine reductase | Autocatalytic | Catalysis | 29 |
| | FGly | C=O | Human sulfatases | Enzymatic (*SUMF*1 FGE) | Catalysis | 30–32 |
| | Sulfenic acid | S–OH | NADH peroxidase/oxidase | Autocatalytic | Catalysis | 33 |
| | | | Nitrile hydratase | Autocatalytic | Catalysis | 34 and 35 |
| | Sulfinic acid | S–OH<br>S=O | Nitrile hydratase | Autocatalytic | Catalysis | |
| | Cys–Heme | C–S | 3-Methyl-L-tyrosine hydroxylase | Autocatalytic | Catalysis | 36 |
| | Methylated | C–S | Methyl-coenzyme M reductase | Enzymatic (MA4545) | Thermal stability, substrate binding | 25–27, 37–39 |
| Cys• | Cys• | | Class II ribonucleotide reductase | Autocatalytic | Regenerate AdoCbl cofactor | 40 |
| Gln | Methylated | C–C | Methyl-coenzyme M reductase | Enzymatic (QCMT) | TBD | 25 and 39 |
| Gly | Thioglycine | C=S | Methyl-coenzyme M reductase | Enzymatic YcaO and TfuA* | Differing opinions based on catalysis or stability | 25, 37 and 38 |
| Gly• | Gly• | | Class III ribonucleotide reductase | Enzymatic (AE) | Generate a transient protein radical, catalysis | 40 |
| | Gly• | | Pyruvate formate lyase | Enzymatic (AE) | Generate a transient protein radical, catalysis | 40 and 41 |
| His | Methylated | C–N | Methyl-coenzyme M reductase | TBD | TBD | 25, 42 and 43 |
| | His–heme | C–N | Cyanobacteria hemoglobin (PCC 6803 and 7002) | Autocatalytic | Catalysis | 44 |
| Ile | Methylated | C–C | Methyl-coenzyme M reductase | TBD | TBD | 42 and 43 |
| Lys | Carboxylated | C–N | Questin oxidase (BTG13) | Autocatalytic | Catalysis | 45 |
| | Carbamylated | C–N | Rubisco | Autocatalytic | Bridging ligand: $Mg^{2+}$ | 46 |
| | | | Urease | Autocatalytic | Bridging ligand: $Ni^{2+}$ | 47 |
| | | | Phosphotriesterase | Autocatalytic | Bridging ligand: $Zn^{2+}$ | 48 |
| | Acetylated | C–N | Acetyl-CoA synthetase | Enzymatic | Regulates activity | 49 and 50 |
| | Ni-pincer-Lys | C–N | Lactate racemase | Enzymatic (LarB, LarC, and LarE) | Catalysis and/or nickel binding | 51 and 52 |
| Met | Oxymethionine | S=O | Methyl-coenzyme M reductase | TBD | TBD | 42 and 43 |
| Ser | Pyruvoyl group | C=O | Histidine decarboxylase | Autocatalytic | Catalysis | 53 and 54 |
| | FGly | C=O | Sulfatase | Enzymatic (AtsB) | Catalysis | 55 and 56 |
| Trp | 7-Hydroxy-Trp | C–O | Methyl-coenzyme M reductase | TBD | TBD | 42 and 43 |
| | 6-Hydroxy-Trp | C–O | Methyl-coenzyme M reductase | TBD | TBD | |
| | Kyn | C=O | Copper binding protein (MbnP) | Enzymatic (MbnH) | Copper binding | 57 |
| | | C=O | Copper-binding protein (MopE*) | TBD | Copper binding | 58 |
| | | C=O | Copper-repressible protein (CorA) | TBD | Copper binding | 59 |
| Tyr | TPQ | C=O | Amine oxidases | Autocatalytic | Catalysis | 60 |
| Tyr• | Tyr• | | Class I ribonucleotide reductase | Autocatalytic | Generate a transient protein radical | 40 |
| | Tyr• | | Photosystem II | Autocatalytic | Catalysis | 61 |
| | Tyr• | | Prostaglandin H synthase | Autocatalytic | Catalysis | 62 |

before the discovery of the pyridinium-3-thioamide-5-thiocarboxylic acid mononucleotide Ni pincer complex, (SCS)Ni(II), in the lactate racemase of *Lactobacillus plantarum* (LarA),[51] such ligands were unknown in biological systems (Fig. 1, **3**). LarA is a nickel-dependent enzyme requiring three auxiliary proteins, LarB, LarC, and LarE, for activation (Fig. 4).[67,68] While the precise roles of these proteins and the mechanism of nickel incorporation were initially unclear, recent studies have elucidated this complex process. Site-directed mutagenesis, coupled with structural analysis, implicated Lys184 in nickel coordination or catalysis, revealing a novel posttranslational modification involving the attachment of a nicotinic acid mononucleotide (NAMN) derivative to its carboxyl group.[51]

A comprehensive investigation of the cofactor biosynthetic pathway jointly by Hausinger and Hu has defined the functions of the three auxiliary proteins starting from a $NAD^+$ precursor, nicotinic acid adenine dinucleotide (NaAD).[52] LarB initiates cofactor assembly by carboxylating and hydrolyzing the pyridine ring of NaAD to yield AMP and pyridinium-3,5-biscarboxylic acid mononucleotide (P2CMN).[69,70] Subsequent reactions with two LarE molecules, involving sacrificial desulfurization of Cys176, convert P2CMN to the thiocarboxylated intermediate, P2TMN.[71–74] LarC purifies with bound nickel,[52] and it is a CTP-dependent nickel-inserting cyclometallase playing the role in nickel insertion into P2TMN and subsequent transfer of the completed (SCS)Ni(II) cofactor to LarA (Fig. 3B).[75]

 

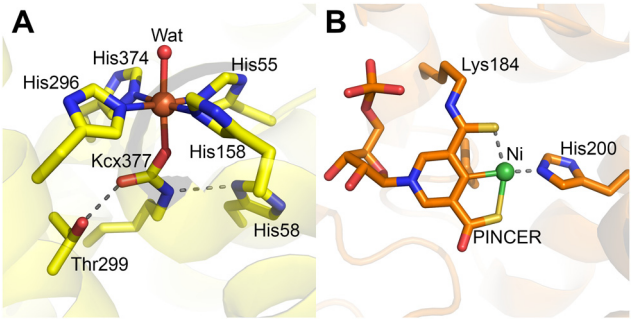


Fig. 3 Crystal structures showing novel lysine PTM's. (A) Iron-binding motif in BTG13 (yellow; PDB 7Y3W) is comprised of four histidine residues, a carboxylated lysine residue, and a water molecule. Thr299 and His58 from the second coordination sphere are shown due to their implications in regulation of Lys377 carboxylation (H-bonding shown in gray dashed lines). (B) Active site of LarA (orange; PDB 4YNS) showing the (SCS)Ni(II) pincer complex with Lys184 and His200 potentially playing roles in catalysis/Ni-binding (coordination shown in gray dashed lines).

The identification of this unprecedented enzyme-generated pincer complex essential for catalyzing the racemization of lactate raises the possibility of similar cofactors in other biological systems. The broad distribution of LarB, LarC, and LarE homologs beyond organisms possessing LarA strongly suggests the potential for additional pincer-dependent enzymes.[51,76]

**2.1.4. Various cofactors in Methyl CoM reductases.** Methyl-coenzyme M reductase (MCR), one of the ten nickel-dependent enzymes[77] catalyzing methane formation in methanogenic archaea,[78] is a rich source of posttranslationally modified amino acids (Fig. 1, **4–14**).[79] Structural studies of MCR in *Methanobacterium thermoautotrophicum* have revealed a cluster of five modified residues near the active site: *S*-methyl-cysteine, 5-C-(*S*)-methyl-arginine, 1-*N*-methylhistidine, 2-C-(*S*)-methyl-glutamine, and thio-glycine.[25] While 5-C-(*S*)-methyl-arginine, 1-*N*-methyl-histidine, and thio-glycine are universally conserved across methanogens, the presence of *S*-methyl-cysteine and 2-C-(*S*)-methyl-glutamine varies among species.[42]

Further investigations of MCR homologs, including ethyl CoM reductase (ECR), MCR from *Methanothermobacter marburgensis*, and MCR from anaerobic methanotrophic archaea (ANME-1), have unveiled a diverse repertoire of novel PTMs. These include 6-hydroxy-tryptophan, 7-hydroxy-tryptophan, didehydro-aspartate, *S*-oxy-methionine, 3-methyl-isoleucine, and 2-*N*-methyl-histidine.[42,43] Notably, didehydro-aspartate, was discovered in MCRs from *M. marburgensis* and *Methanosarcina barkeri* through peptide-sequencing and mass spectrometry and confirmed by a 2.15 Å resolution crystal structure.[27] The formation of the double bond in didehydro-aspartate restricts the conformational space of the side chain, reducing the mobility of the carboxylate group and decreasing the residue's p$K_a$. It is proposed that this modification fine-tunes enzyme structure to optimize substrate-binding and catalysis.[27]

The distribution of these modifications varies across different MCRs. For example, ANME-1 harbors 7-hydroxy-tryptophan and *S*-oxymethionine,[80] while MCR from *Methanotorris formicicus* contains 6-hydroxy-tryptophan.[81] 3-Methyl-isoleucine and 2-*N*-methyl-histidine have been identified in the structure of *Candidatus* Ethanoperedens thermophilum MCR.[82] The non-overlapping occurrence of 7-hydroxy-tryptophan and methylated

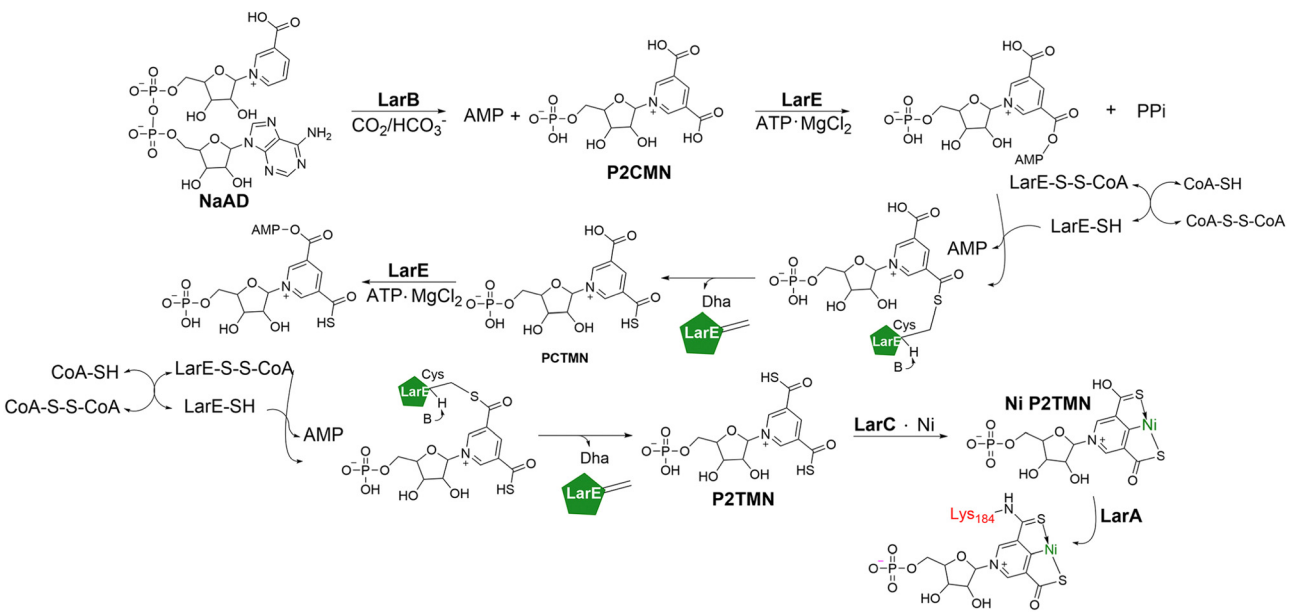


Fig. 4 Proposed biogenesis mechanism of (SCS)Ni(II) pincer complex. LarB is responsible for the formation of P2CMN from NaAD in a $CO_2$/bicarbonate dependent reaction. Two LarE molecules are required for P2TMN formation. LarE activates P2CMN *via* adenylylation, covalently links the protein to P2CMN, and sacrifices a sulfur atom from its own cysteine residue to form the thioacid of P2CMN, a second LarE protomer repeats the set of reactions, where Dha is released as a product upon sulfur atom donation, forming P2TMN. LarC is suggested to be responsible for Ni insertion into P2TMN and transferring the cofactor to LarA (the straight arrow in the pincer indicates coordination).

arginine in ANME-1 suggests potential compensatory functions for these modifications.[80] Similarly, 6-hydroxy-tryptophan may compensate for the absence of didehydro-aspartate in MCR.[81] However, the precise roles and biosynthetic origins of many of these PTMs remain to be fully elucidated.

Significant progress has been made in understanding the biosynthesis of *S*-methyl-cysteine, 2-C-(*S*)-methyl-glutamine, 5-C-(*S*)-methyl-arginine, and thio-glycine.[83] Gene knockout studies on the α subunit of MCR (McrA) have shown that the *ycaO-tfuA* locus is required for thio-glycine formation, where phylogenetic analyses showed their prevalence in methanogens.[37] Thio-glycine, present in all examined MCRs, is implicated in stabilizing secondary protein structure near the active site, although its formation mechanism is still under investigation.[37] A SAM-dependent methyltransferase, encoded by *mcmA*, is hypothesized to be responsible for the methyl-cysteine modification.[38] Studies on MCR mutants lacking thio-glycine and methyl-cysteine showed significant growth defects, suggesting a synergistic interaction between these two modifications.[38] While histidine methylation is conserved in all methanogens, the specific enzyme remains unidentified, although a SAM-dependent methyltransferase is suspected. It is hypothesized that this methylation positions the imidazole that coordinates coenzyme B, CoB.[84]

The methylation of arginine in MCR is catalyzed by the radical SAM methyltransferase MA4551 (Mmp10), also known as arginine C-methyltransferase (RCMT).[26] RCMT utilizes methylcobalamin (MeCbl) as a cofactor.[26,85] Booker *et al.* classified *Ma*Mmp10 (Mmp10 from *Methanosarcina acetivorans*) as a new member of subclass B in the radical SAM methyltransferase family, revealing a C-terminal cobalamin-binding domain.[86] EPR studies have shown that a tyrosine residue coordinates the [4Fe–4S] cluster, enabling both radical and nucleophilic chemistry,[85] similar to the initial steps of tyrosine cleavage by HydG of the radical SAM superfamily[87,88] for cyanide production.[89,90] The proposed mechanism involves SAM binding, assisted by tyrosine displacement in the [4Fe–4S] cluster. The 5′-deoxyadenosyl radical abstracts a hydrogen atom from arginine, initiating methyl transfer from MeCbl.[85] The resulting Co(II) intermediate is likely reduced back to MeCbl by a ferredoxin (Fig. 5). Similarly, glutamine methylation in MCR is catalyzed by an enzyme of class B radical SAM methyltransferases, glutamine C-methyltransferase (QCMT), which utilizes a [4Fe–4S] cluster and MeCbl similarly. Studies have shown that QCMT transfers a methyl group from SAM to cobalamin(I), regenerating MeCbl, with 5′-deoxyadenosine and *S*-adenosyl-L-homocysteine as co-products.[38,91] The similarities between QCMT and RCMT suggest analogous catalytic mechanisms.

Intriguingly, the methylation of glutamine in MCR is also catalyzed by a class B radical SAM methyltransferase, termed glutamine C-methyltransferase (QCMT).[39] Using the putative QCMT from *Methanoculleus thermophilus*, Layer *et al.* demonstrated glutamine methylation in an MCR-derived peptide substrate.[39] QCMT possesses a single [4Fe–4S] cluster and enzyme-bound MeCbl cofactor utilized during catalysis. UV-vis spectra and HPLC analysis indicated that SAM was transferring a methyl group to cobalamin(I), regenerating MeCbl. A QCMT reaction with a peptide substrate revealed the presence of two co-products, 5′-deoxyadenosine and *S*-adenosyl-L-homocysteine.[39] Due to the significant similarities in QCMT and RCMT, it is assumed that

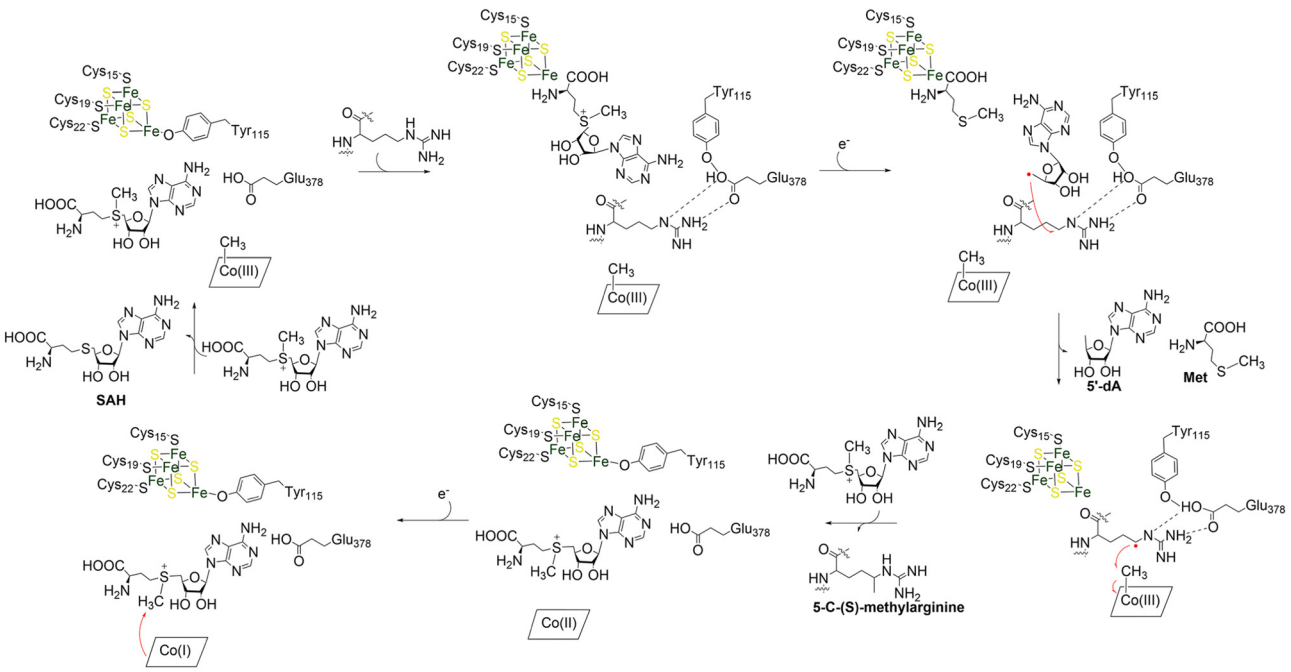


Fig. 5 Proposed catalytic cycle of arginine C-methyltransferase (RCMT), also known as Mmp10, to produce 5-C-(*S*)-methylarginine, methionine, 5′-deoxyadenosine, and *S*-adenosyl-L-homocysteine.[85]

 

they catalyze similar reactions to methylate their corresponding residues.

**2.1.5. Kynurenine formation from tryptophan.** Methanobactins (Mbns) are ribosomally synthesized and posttranslationally modified natural products with a high affinity for Cu(I), utilized by methanotrophs as a copper source.[92] While many proteins encoded by Mbn operons have assigned functions, the roles of MbnP, a tryptophan-rich protein, and MbnH, a diheme cytochrome *c* peroxidase (C*c*P), remained unclear until recently.[57,92] MbnH belongs to the (bC*c*P)/MauG family, of which MauG catalyzes tryptophan tryptophylquinone (TTQ) formation in pre-methylamine dehydrogenase (preMADH)[93–95] *via* a free radical approach[96,97] mediated by a reactive *bis*-Fe(IV) intermediate[98] in long-range remote catalysis (which will be discussed in Section 3.1).[96,99–102] Notably, MbnH exhibits a charge resonance (CR) near-infrared band upon reaction with hydrogen peroxide, a spectroscopic signature associated with the *bis*-Fe(IV) intermediate of MauG, indicating a through-space stabilization of the high-valent *bis*-Fe(IV) centers.[99,100,103,104] A 2.09 Å resolution crystal structure of MbnP$^{H}$, (MbnP coexpressed with MbnH), revealed a copper-binding site containing histidine, methionine, solvent-derived ligand, and kynurenine at residue 174 (Kyn174), a tryptophan-derived cofactor generated by oxygenation of a tryptophan residue (Fig. 1, 15).[57] Kyn174 is a protein-bound residue, distinct from endogenous kynurenine that is present in the body as a metabolic intermediate in the major catabolic pathway of tryptophan.[100,105–108] Trp174, the precursor to Kyn174, is part of a conserved WxW motif in MbnP proteins.[57] Mutation of Trp174 to tyrosine significantly reduced copper binding, demonstrating the importance of the kynurenine cofactor for copper association.[57] Although kynurenine is also present in the copper-binding sites of MopE* and CorA, these proteins adopt distinct structural folds (Fig. 6).[57–59] In all three proteins, the copper–kynurenine distance exceeds typical Cu–N bond lengths, suggesting that kynurenine is not directly coordinated with the copper ion.[57] Further studies are needed to elucidate the mechanism of kynurenine formation from a tryptophan residue and the biological function of these proteins.

**2.1.6. Tyrosine modification in copper amine oxidases: 2,4,5-trihydroxyphenylalanine quinone (TPQ) and lysine tyrosylquinone (LTQ).** Copper amine oxidases (CuAOs) are homodimeric enzymes that catalyze the $O_2$-dependent oxidation of primary amines to aldehydes, with the concomitant production of ammonia and $H_2O_2$ through a ping-pong kinetic mechanism.[109] These enzymes are widespread, participating in diverse biological processes such as cell growth, apoptosis, and hormone biosynthesis.[109] Known as quinoproteins, CuAOs utilize covalently linked cofactors—2,4,5-trihydroxyphenylalanine quinone (TPQ) (Fig. 1, **16**) or lysine tyrosylquinone (LTQ) (Fig. 1, **26**)—to facilitate catalysis. These quinone moieties are derived from tyrosine residues through an autocatalytic process that depends on copper and molecular oxygen.[60,110]

The TPQ cofactor was first identified in 1990 *via* biochemical studies and later confirmed by X-ray crystallography (Fig. 7A). Structural insights have been obtained from bacteria, plant, and mammal CuAOs, providing a comprehensive understanding of their catalytic mechanisms.[111–117] Notably, the copper amine oxidase from *Arthrobacter globiformis* (AGAO) has been extensively studied to elucidate the stepwise formation of TPQ. Apo-AGAO crystals which feature an unmodified tyrosine residue Tyr382, were soaked in $CuSO_4$ and exposed to an oxygen-saturated buffer to monitor TPQ (Fig. 8).[118]

The first step in TPQ formation involves the binding of a copper(II) ion to the protein, positioning it approximately 2.5 Å from the hydroxyl group of Tyr382. Upon exposure to oxygen for 10 minutes, an O atom was detected near the C3 position of the tyrosine ring, with an occupancy of 0.5.[118] This observation suggested the presence of a transient intermediate comprising both the unmodified tyrosine and its partially oxidized quinone form, referred to as dopaquinone (DPQ).[118]

Prolonged exposure to oxygen for 100 minutes revealed another intermediate lacking the characteristic 480 nm absorption peak of fully mature TPQ. This intermediate exhibited two oxygen atoms near the C2 and C5 positions of the tyrosine ring, consistent with the reduced form of TPQ ($TPQ_{red}$).[118] Since mature TPQ contains oxygen atoms at the C2, C4, and C5 positions, the previously observed oxygen at C3 in DPQ likely corresponds to C5 in $TPQ_{red}$, implying a 180° rotation of the quinone ring during maturation.

The final step involves the oxidation of $TPQ_{red}$ by a second molecule of molecular oxygen, yielding the fully mature

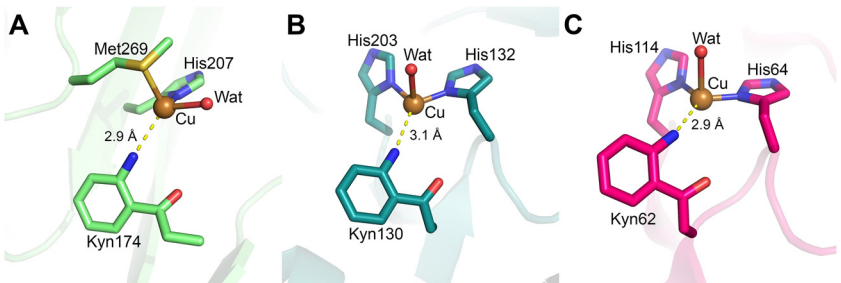


Fig. 6 Active sites of copper-binding proteins containing kynurenine. (A) The copper ion in MbnP$^{H}$ (light green; PDB 7L6G) is coordinated in a tetrahedral geometry by a methionine, histidine, kynurenine, and a water molecule. (B) The copper ion in MopE* (turquoise; PDB 2VOV) is coordinated by two histidine residues, kynurenine and a water molecule. (C) CorA's copper ion (pink; PDB 4BZ4) is also coordinated by two histidine residues, kynurenine, and a water molecule.

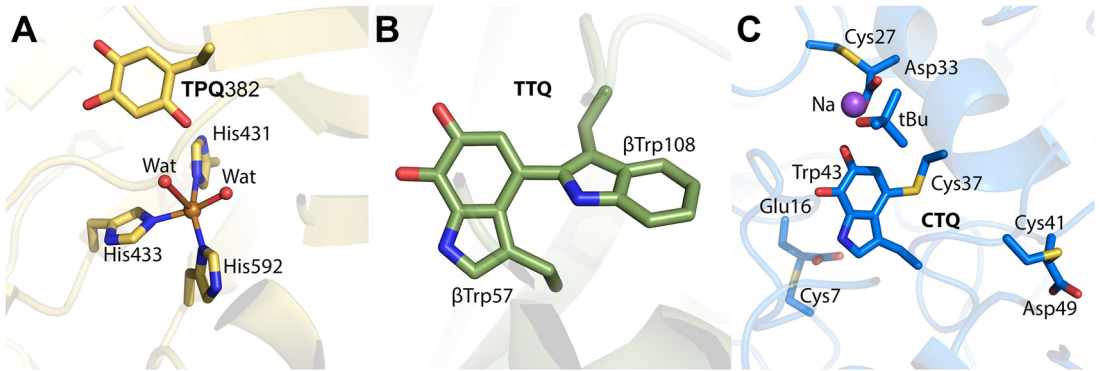


Fig. 7 Crystal structures of cofactors in present in quinoproteins. (A) Amine oxidase of *A. globiformis* with mature TPQ cofactor (yellow; PDB 1IVX). The copper center is coordinated in a distorted square-pyramidal geometry by two water molecules and three histidine residues. (B) Wild-type MauG in complex with pre-MADH crystals aged 130 days, showing the crosslink between β-Trp57 and β-Trp108 (green; PDB 4FA1). (C) CTQ in the γ-subunit of QHNDH from *Pseudomonas putida* (blue; PDB 1JMX). Cys7, Cys27, and Cys41 of the γ-subunit are involved in thioether crosslinks with Asp or Glu residues that surround the CTQ cofactor.

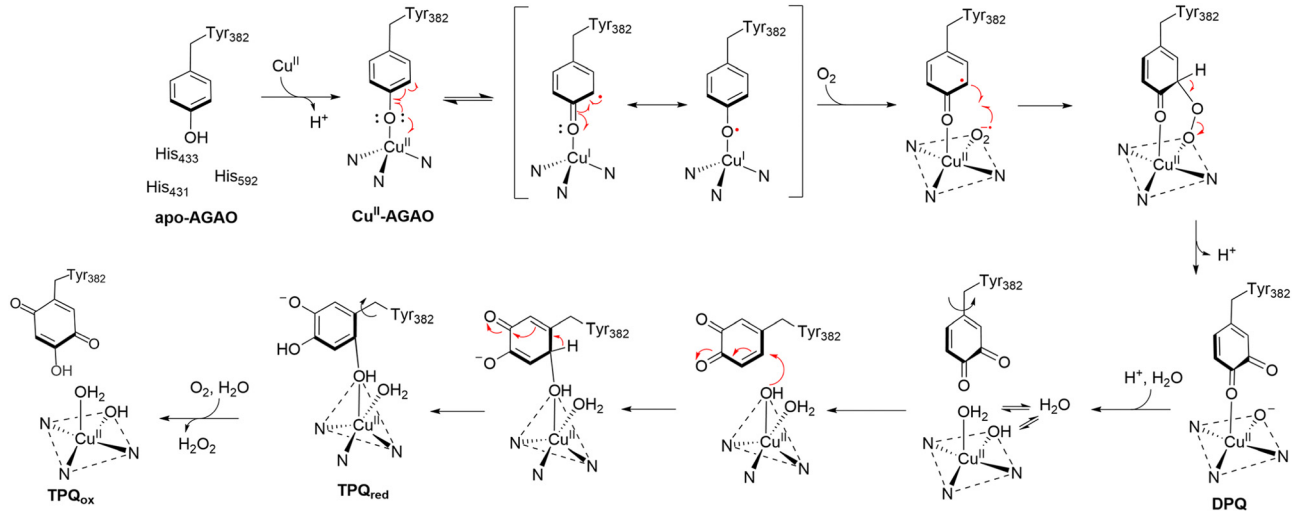


Fig. 8 Proposed mechanism of formation of TPQ in AGAO.[118] Crystal structures for apo-AGAO, Cu$^{II}$-AGAO, DPQ, TPQ$_{red}$, and TPQ$_{ox}$ have been characterized and published with PDB codes 1AVK, 1IVU, 1IVV, 1IVW, and 1IVX, respectively.

oxidized form of TPQ (TPQ$_{ox}$) and $H_2O_2$.[118,119] This sequential mechanism highlights the intricate interplay between copper coordination, tyrosine oxidation, and ring conformational changes during TPQ biogenesis.

By contrast, LTQ biogenesis involves a crosslink between lysine and tyrosine residues, forming a distinct quinone cofactor, which will be further discussed in Section 3.3. Although less studied than TPQ, LTQ plays a similarly essential role in enabling CuAO catalysis and warrants further exploration to delineate its formation and function in enzymatic systems.

The catalytic mechanism of CuAOs has been studied, revealing a two-step process comprising a reductive half-reaction and an oxidative half-reaction (Fig. 9). In the reductive phase, the primary amine substrate is oxidized to an aldehyde, while TPQ is reduced. The oxidative half-reaction regenerates TPQ, releasing $NH_3$ and $H_2O_2$ as byproducts.[120]

A recent study provided new insights into the dynamic conformational changes during catalysis through *in crystallo* thermodynamic analysis of noncryocooled AGAO crystals.[120] TPQ exists in two major conformations: the "off-copper" state, where it is distant from the copper(II) ion, and "on-copper" state, where it coordinates with the metal center and is catalytically active. During the reductive half-reaction, TPQ is reduced by the substrate to its aminoresorcinol form (TPQ$_{amr}$) which resides in the off-copper state. This form is in equilibrium with the on-copper semiquinone radical (TPQ$_{sq}$).[120]

Murakawa and colleagues ingeniously employed the humid air and glue-coating (HAG) method, commonly used in non-cryogenic crystallography, to investigate the temperature-dependent behavior of TPQ. Using anaerobically substrate-soaked AGAO crystals, they demonstrate that increasing temperature facilitates the transition from TPQ$_{amr}$ to TPQ$_{sq}$.

 

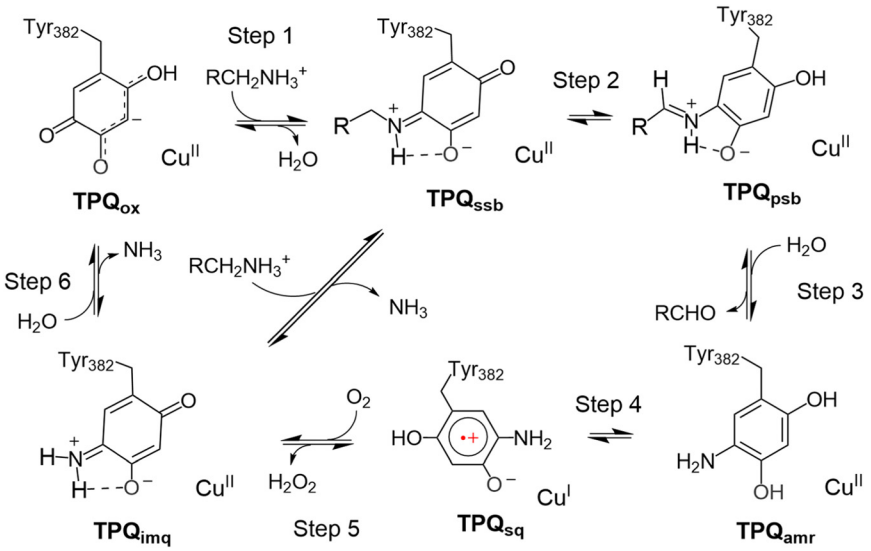


Fig. 9 Proposed catalytic mechanism of CuAOs. Steps 1–4 belong to the reductive half-reaction and the remaining steps are the oxidative half-reaction.[120] $TPQ_{ox}$, fully oxidized TPQ; $TPQ_{ssb}$, TPQ substrate Schiff-base; $TPQ_{psb}$, TPQ product Schiff-base; $TPQ_{amr}$, TPQ aminoresorcinol form; $TPQ_{sq}$, TPQ semiquinone radical, the "on-copper" catalytically active conformation, TPQ semiquinone form; $TPQ_{imq}$, TPQ iminoquinone form.

This transition was further corroborated by single-crystal UV-vis spectroscopy, providing direct evidence of temperature-mediated conformational equilibrium.[98] These findings emphasize the sophisticated interplay of cofactor conformation, substrate interactions, and environmental conditions in CuAO catalysis, offering deeper insights into the mechanistic versatility of protein-derived cofactors.

### 2.2. One oxidation state up: single amino acid residues harboring paramagnetic free radicals as cofactors

Free radicals on amino acid residues represent a unique class of protein-derived cofactors, serving as catalytic driving forces in diverse enzymatic systems. This section explores the biogenesis, stabilization, and functional roles of these radicals.

**2.2.1. Stable tyrosyl radical.** The discovery of a stable tyrosyl radical in *Escherichia coli* ribonucleotide reductase (RNR) revolutionized the understanding of free radicals in enzymology, demonstrating that radicals can be both highly stable and integral to catalysis. First identified in the R2 subunit in 1972 as a built-in organic radical required for enzyme activity with a sharp absorbance at 410 nm and a doublet splitting EPR signal at $g = 2.0047$,[121] a stable tyrosyl free radical cofactor in the protein was discovered,[122–124] expanding the field of radical enzymology.[124–126] The tyrosyl radical has remarkable stability, persisting for days at room temperature if the protein remains intact.[123]

This radical is formed during protein synthesis *via* an autocatalytic process involving a diiron cluster. Oxygen reacts with the diiron center to form a mixed-valence Fe(III)–O–Fe(IV) intermediate,[127–129] which oxidizes a nearby tyrosine residue, yielding the tyrosyl radical while reducing the diiron cluster to the diferric state. The hydrophobic pocket surrounding the diiron center and the local electrostatic environment provide a protective environment that stabilizes the radical.[130,131]

The catalytic role of the tyrosyl radical becomes evident upon interaction with the R1 subunit. When R1 binds its substrate, a ribonucleotide diphosphate, the two subunits form a complex,[132] enabling the transfer of oxidizing power from the R2 subunit's tyrosyl radical through a hydrogen-bonded network to the active site in R1. This generates a cysteine thiol radical that initiates substrate reduction.[133,134] Following each turnover, the tyrosyl radical is regenerated, demonstrating its role as a true catalytic cofactor.[135]

Beyond RNRs, tyrosyl radicals as protein-derived cofactors play significant roles in other systems, such as photosystem II (PSII) and prostaglandin H synthase (PGHS).[136] In PSII, two tyrosyl radicals, $Y_Z^{\bullet}$ and $Y_D^{\bullet}$, contribute distinct functions in water-splitting catalysis. $Y_Z^{\bullet}$ mediates electron transfer to $P680^+$ in the photosynthetic electron transport chain, rapidly reduced back to tyrosine and oxidized to the radical state. Conversely, $Y_D^{\bullet}$ is exceptionally stable, persisting for minutes to hours, and is believed to assist in assembling and stabilizing the oxygen-evolving complex.[137,138] Computational studies have revealed that $Y_D^{\bullet}$'s stability is linked to a water-mediated proton transfer pathway within its hydrophobic environment, explaining its slower oxidation kinetics.[139] PGHS is a heme-dependent bifunctional enzyme, a tyrosyl radical plays an active role in the cyclooxygenase activity that initiates prostaglandin biosynthesis.[140–142] The radical is generated during catalysis and accumulates alongside product formation, signifying its central role in the reaction mechanism. These examples underscore the versatility and adaptability of tyrosyl radicals as catalytic cofactors in diverse enzymatic systems.

**2.2.2. Stable glycyl radical.** Glycyl radicals are critical to the catalytic activity of enzymes involved in anaerobic metabolism, such as pyruvate formate lyase (PFL) and anaerobic RNRs (class III RNRs).[143–148] These radicals are generated by activating enzymes (termed activases) containing Fe–S clusters, which

produce a 5′-deoxyadenosyl radical from *S*-adenosyl methionine.[149] A $Zn(Cys)_4$ center is present in the catalytic subunit of anaerobic RNR, and its absence through mutation is shown to inactivate the enzyme as the result of their inability to generate the catalytically essential glycyl radical although the mechanism of which requires further investigation.[150] This radical abstracts a hydrogen atom from a glycine residue, creating a catalytically active glycyl radical.[151–153] Glycyl radicals in these enzymes have demonstrated permanent stability under strict anaerobic conditions.[147,148] However, glycyl radicals are extremely oxygen-sensitive, resulting in peptide cleavage at the radical site and enzyme inactivation upon exposure.[41,146,154] In PFL and class III RNR, the glycyl radical is transferred to a cysteine residue, generating a catalytic thiyl radical essential for pyruvate cleavage or nucleotide diphosphate reduction.[40,153,155]

Other enzymes containing glycyl radicals include glycerol dehydratase, benzylsuccinate synthase, and hydroxyphenylacetate decarboxylase.[153] Collectively termed glycyl radical enzymes (GREs), they share a common mechanism of radical transfer to cysteine residues for catalytic activity. Stabilization and precise transfer mechanisms of glycyl radicals remain active areas of research.

**2.2.3. Transient thiyl and tryptophanyl radicals.** It is debatable whether transient amino acid radicals mediating catalysis should be formally classified as protein-derived cofactors. While they are crucial for enzyme function and are generated within the protein itself, their transient nature distinguishes them from more stable protein-derived cofactors like permanently stable tyrosyl radicals in RNR or PSII. Therefore, while these radicals are important for enzyme catalysis and should be discussed, they may not always be explicitly listed alongside other, more stable protein-derived cofactors in a comprehensive overview such as Fig. 1.

Thiyl radicals are essential to the catalytic mechanisms of RNRs, which play a central role in DNA synthesis. All RNR classes employ a transient thiyl radical to initiate nucleotide reduction, with variations in its generation mechanisms.[144,156–163] To kinetically and spectroscopically study the elusive thiyl radical, researchers have utilized selenocysteine substitution.[164] With its lower $pK_a$ and reduction potential, selenocysteine enhances radical stabilization, facilitating detection and advancing the understanding of thiyl radicals in enzymatic catalysis.[165]

Tryptophan radical cations are exemplified by cytochrome *c* peroxidase (C*c*P), a heme-dependent enzyme that catalyzes the oxidation of Fe(II)-cytochrome *c* to Fe(III)-cytochrome *c* while reducing $H_2O_2$ to water.[166] The key intermediate is $Trp191^{\bullet+}$,[167] which facilitates long-range electron transfer to its substrate, cytochrome *c*.[168–170] Structural and spectroscopic studies reveal that protein environments, such as solvent accessibility and proximal charges, critically influence the stability of $Trp^{\bullet+}$.[171] For example, the presence of a nearby cation-binding site in ascorbate peroxidase (APX) leads to the stabilization of a porphyrin π-cation radical instead of a $Trp^{\bullet+}$.[172,173] However, in *Leishmania major* C*c*P (LmP), a $Trp^{\bullet+}$ radical forms despite the presence of a similar cation-binding site, suggesting that solvent environment differences may play a significant role.[174] Recent computational studies have investigated the factors governing $Trp^{\bullet+}$ stabilization, highlighting the roles of protein structure and solvent interactions.[175] Despite substantial progress, questions remain about why C*c*P favors a $Trp^{\bullet+}$ over a porphyrin radical and how this radical is reduced during catalysis.

# 3. Protein cofactors derived from the covalent crosslink of two amino acids

Covalent crosslinking between two amino acid residues forms a unique class of protein-derived cofactors, which play crucial roles in enhancing enzyme catalysis by creating specialized active sites with new redox centers. Among these cofactors, eight distinct types have been characterized to date, including Cys–His, Cys–Lys, Cys–Tyr, Cys–Trp, His–Tyr, Lys–Tyr, oxygenated Trp–Trp, and the radical form of $(Cys–Tyr)^{\bullet}$ (Table 2). These crosslinked cofactors exhibit unique structural and functional properties, often arising through intricate biosynthetic pathways. This section examines these cofactors in detail, with a focus on their structural features, catalytic roles, and the underlying mechanisms of their formation.

## 3.1. Tryptophan modification in amine dehydrogenases: tryptophan tryptophylquinone (TTQ)

The protein-derived cofactors accommodated by quinoproteins are among the most well-studied in terms of mechanisms of formation. Currently, five amino acid crosslinked cofactors with quinone moieties have been identified as redox centers in enzymes.[22] These are:

- Cysteine tryptophylquinone (CTQ, Fig. 1, **25**) in quinohemoprotein amine dehydrogenase (QHNDH),[60,110,183,197,200,201] L-lysine ε-oxidase (LodA),[202] and glycine oxidase (GoxA).[185]
- Lysine tyrosylquinone (LTQ, Fig. 1, **26**) in lysyl oxidase.[110]
- Pyrroloquinoline quinone (PQQ, **37** in Fig. 1, **37**)[203] in alcohol dehydrogenases and aminoadipic 6-semialdehyde dehydrogenase.[204,205]
- 2,4,5-Trihydroxyphenylalanine quinone (TPQ, Fig. 1, **16**) in amine oxidases.[60]
- Tryptophan tryptophylquinone (TTQ, Fig. 1, **24**) in methylamine dehydrogenase.[197–199]

Among them, the biogenesis of TTQ is well studied. This quinone cofactor formed through the crosslinking and subsequent oxygenation of two tryptophan components (Fig. 1, **24**). TTQ is the hallmark cofactor of methylamine dehydrogenase (MADH), an enzyme that catalyzes the oxidation of methylamine to formaldehyde and ammonia.[197] TTQ serves as a prime example of how protein-derived cofactors confer remarkable catalytic capabilities, enhancing substrate specificity and turnover efficiency. The formation of TTQ involves a sophisticated posttranslational modification pathway, mediated by the diheme enzyme MauG.[206,207]

MauG must handle a large substrate with specificity. The biogenesis of TTQ is accomplished in a 119 kDa cofactor-free

 

Table 2 Protein cofactors derived from the covalent crosslink of two amino acids

| Source | Cofactor | New chemical bonds formed | Representative enzyme | Biogenesis | Function | Ref. |
|---|---|---|---|---|---|---|
| Cys–His | Cys–His | C–S | Tyrosinase | Autocatalytic | TBD | 23 and 176–178 |
| | Cys–His | | Hemocyanin | Autocatalytic | TBD | 23, 179 and 180 |
| | Cys–His | | Catechol oxidase | Autocatalytic | TBD | 23 and 181 |
| Cys–Lys | NOS bridge | N–O–S | Transaldolase | Autocatalytic | Allosteric redox switch | 182 |
| Cys–Trp | CTQ | C–S | Quinohemoprotein amine dehydrogenase (QHNDH) | Enzymatic (QhpG, QhpA) | Catalysis | 183 |
| | | | L-Lysine-ε-oxidase (LodA) | Enzymatic (LodB) | Catalysis | 184 |
| | | | Glycine oxidase (GoxA) | Enzymatic (GoxB) | Catalysis | 185 |
| (Cys–Tyr)• | (Cys–Tyr)• | C–S | Galactose oxidase | Autocatalytic | Catalysis | 186 and 187 |
| Cys–Tyr | Cys–Tyr | C–S | Cysteine dioxygenase | Autocatalytic | Catalytic Amplifier | 188 |
| | Cys–Tyr | | Cysteamine dioxygenase | Autocatalytic | Catalytic Amplifier | 12 |
| | Cys–Tyr | | Copper radical oxidase (GlxA) | Autocatalytic | Catalysis | 189 |
| | Cys–Tyr | | Sulfite reductase (NirA) | Autocatalytic | Catalysis | 190 |
| | Cys–Tyr | | Putative zinc protease (BF4112) | Autocatalytic | Catalysis (putative) | 15 |
| | Cys–Tyr | | Cytochrome *c* nitrite reductase (TvNiR) | Autocatalytic | Catalysis | 191 |
| His–Tyr | His–Tyr (a) | aromatic C–N | Cytochrome *c* oxidase | Autocatalytic | Copper binding | 192–194 |
| | His–Tyr (b) | $C_\beta$–N | Catalase | TBD | TBD | 195 and 196 |
| Lys–Tyr | LTQ | C–N | Lysyl oxidase | Autocatalytic | Catalysis | 110 |
| Trp–Trp | TTQ | C–C | Methylamine dehydrogenase (MADH) | Enzymatic (MauG) | Catalysis | 197–199 |

precursor protein, preMADH, containing two tryptophan residues at positions critical for cofactor assembly.[93] MauG catalyzes the oxidative maturation of these residues into TTQ *via* a six-electron oxidation process (Fig. 10).[97,102] The oxidant in this system, $H_2O_2$, interacts with the deeply buried hemes of MauG, initiating a cascade of high-energy intermediates.

Upon binding $H_2O_2$, the distal heme of MauG undergoes oxidation to form an Fe=O species coupled with a porphyrin radical. The oxidizing equivalent is then transferred to the proximal heme, generating a *bis*-Fe(IV) intermediate.[98] This *bis*-Fe(IV) species is remarkably stable in the absence of preMADH, persisting for hours due to a biological charge resonance (CR) stabilization mechanism.[99,100] This stabilization is characterized by a near-infrared (NIR) absorption band with maxima at 950–960 nm, a phenomenon rarely observed in biological systems. Unlike the short-lived ferryl intermediates that typically oxidize small-molecular substrates, the exceptional stability of *bis*-Fe(IV) in 43 kDa MauG enables the intermediate to oxidize a large substrate of 119 kDa preMADH on its specific two tryptophan residues (one is an already hydroxylated 7-OH-Trp) through long-range remote catalysis.[96,101]

The *bis*-Fe(IV) intermediate serves as the catalytic linchpin for oxidizing the tryptophan residues in preMADH.[98] Despite the physical separation (~40 Å) between MauG's catalytic center and the substrate tryptophans, the oxidation proceeds through a long-range electron transfer mechanism.[102] This transfer is facilitated by a network of aromatic residues in MauG and involves a hole-hopping pathway *via* a surface-exposed tryptophan residue.[101] The oxidative modification of preMADH occurs across an approximately 40 Å interface between the $H_2O_2$-binding site in MauG and the TTQ formation site in preMADH, producing a diradical of Trp• and (Trp-OH)• for crosslinking,[96] exemplifying the efficiency of biological electron transfer mechanisms.

Each TTQ assembly cycle involves the consumption of one $H_2O_2$ molecule, repeating three times to deliver the six required oxidizing equivalents. During each cycle, MauG's *bis*-Fe(IV) intermediate oxidizes one target tryptophan residue in

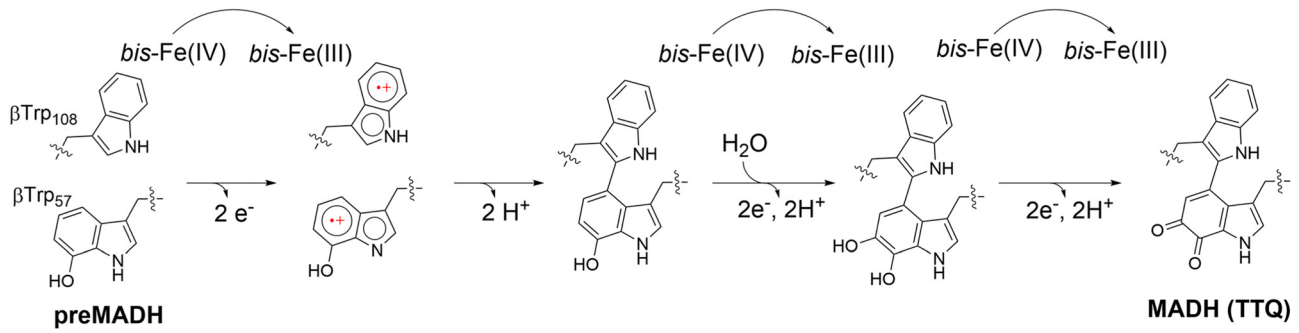


Fig. 10 Proposed biogenesis mechanism of TTQ in MADH.[96] TTQ maturation in MauG-preMADH crystals with slow release of $H_2O_2$ of the cryoprotectant illustrates TTQ formation, showing that the crosslink between the two Trp residues occurs prior to the addition of a second oxygen atom. The PDB codes for aged crystal structures are 4FA4, 4FA5, 4FA9, 4FAN, 4FAV, and 4FA1, in ascending order.

preMADH. The modifications include hydroxylation, crosslink formation, and further oxidation to achieve the mature TTQ structure.[96] This cumulative oxidative process transforms preMADH into catalytically active MADH, equipped with a fully formed TTQ cofactor (Fig. 7B).

### 3.2. Cysteine tryptophylquinone (CTQ)

CTQ is a quinone cofactor derived from the crosslinking of cysteine and tryptophan residues (Fig. 1, **25**).[208] It has been identified in various enzymes, including quinohemoprotein amine dehydrogenase (QHNDH)[183] L-lysine ε-oxidase (LodA),[202] and glycine oxidase (GoxA),[185] where it plays a crucial role in the oxidation of primary amines or amino acids to their corresponding aldehydes or keto acids. These enzymatic reactions are significant in energy metabolism and catabolism, demonstrating the versatility and catalytic efficiency of CTQ-containing enzymes.

QHNDH is a diheme enzyme that catalyzes the oxidation of primary amines to aldehydes, with energy generation as a byproduct. Its CTQ cofactor is formed during a multistep biosynthetic process involving several auxiliary proteins. The flavoprotein monooxygenase QhpG plays a central role in catalyzing the final oxidation step to form the mature CTQ (Fig. 7C) from the precursor peptide encoded by the *qhpC* gene, which forms the γ-subunit of QHNDH. However, this final step is preceded by sequential modifications orchestrated by QhpD and QhpE.[209]

QhpD mediates the formation of three Cys-to-Asp/Glu thioether bonds within the QhpC polypeptide, a step critical for stabilizing the cofactor's nascent structure. Structural studies revealed that QhpG preferentially binds to a QhpCD binary complex, facilitating efficient CTQ formation. This hierarchical assembly and multienzyme coordination are reminiscent of TTQ biogenesis in methylamine dehydrogenase (MADH), which similarly involves a diheme enzyme (MauG) to oxidize precursor tryptophan residues.

In L-lysine ε-oxidase (LodA) and glycine oxidase (GoxA), CTQ synthesis occurs *via* distinct pathways. Unlike the diheme protein-dependent biogenesis seen in QHNDH, LodA and GoxA rely on flavoproteins, LodB and GoxB, respectively, to generate their cofactors.[184,185,202,210] These differences suggest unique evolutionary adaptations and mechanistic diversity among CTQ-bearing enzymes. Comparative studies have highlighted variations in the roles and structural contexts of CTQ within these systems, emphasizing the need for further research to delineate the precise biogenesis and catalytic mechanisms across different enzyme classes.

CTQ exemplifies the biochemical ingenuity of quinone cofactors in enzymology, showcasing the versatility of protein-derived modifications in facilitating challenging redox reactions. Its formation and function differ across enzyme families, illustrating how protein environments and accessory proteins adapt to specific biochemical needs. For a comprehensive overview of quinone cofactors, readers are directed to the detailed review by Klinman and Bonnot, which delves into the biogenesis and functionality of these remarkable molecular motifs.[22] The formation and stabilization of these crosslinked quinone cofactors underscore the evolutionary creativity of enzymes in harnessing free radical chemistry and long-range electron transfer for catalysis. As research advances, further insights into the structural determinants and dynamic pathways governing CTQ and TTQ biogenesis will continue to inspire biomimetic and synthetic applications.

### 3.3. Lysine tyrosylquinone (LTQ)

The quinone moiety of LTQ is also derived from a tyrosine residue. However, in addition to the tyrosine modification, there is also a crosslink between the quinone tyrosine and the side chain nitrogen of a lysine residue (Fig. 1, **26**). LTQ was first identified and characterized through the biochemical investigation of a peptide from bovine aorta lysyl oxidase (LOX), a protein responsible for the posttranslational modification of elastin and collagen in the metabolism of connective tissue.[110] Reminiscent of TPQ, the formation of LTQ is also a copper and oxygen-dependent autocatalytic process, and is required for catalysis. Due to its membership in the CuAO family, it is assumed that the mechanism of formation of LTQ is similar to that of TPQ, but with the addition of the lysine nitrogen into the orthoquinone intermediate.[4] A 2.4 Å resolution crystal structure of human lysyl oxidase-like 2 (hLOXL2) has a zinc ion occupying the copper-binding site, which prevented LTQ formation but the LTQ forming residues were observed 16.6 Å away from each other, suggesting that the published structure is in a precursor state to LTQ formation.[211] The structure of the mature LOXL2 containing the LTQ cofactor is predicted through molecular modeling and simulations.[212] However, a crystal or cryo-EM structure of LOX with a mature LTQ cofactor has yet to be determined experimentally.

### 3.4. Cys–Lys crosslink with a NOS bridge in transaldolase

Transaldolase, a pivotal enzyme in the pentose phosphate pathway across all domains of life, has garnered significant attention as a potential drug target. Recent studies by Tittman and colleagues on the transaldolase enzyme of *Neisseria gonnorhoeae* (*Ng*TAL) has revealed an unprecedented redox-regulated mechanism mediated by a unique protein-derived cofactor (Fig. 1, **27**).[182] This discovery underscores the enzyme's potential as a therapeutic target for combating gonorrhea, a sexually transmitted disease of global concern.

The study demonstrates that *Ng*TAL's enzymatic activity is modulated by redox conditions. Site-directed mutagenesis of its three cysteine residues revealed that none of these form disulfide bonds, yet the loss of redox regulation upon substitution of Cys38 pointed to its critical role. Structural characterization of the oxidized and reduced states of *Ng*TAL provided further insights. In the reduced state, *Ng*TAL exhibits catalytic activity, while in the oxidized state, activity is abolished. Crystallographic analyses of the oxidized form unveiled a novel covalent crosslink between Cys38 and Lys8, bridged by an additional oxygen atom—forming an NOS (nitrogen–oxygen–sulfur) bridge (Fig. 11B). This crosslink is absent in the reduced state (PDB 3CLM), wherein molecular oxygen is observed near Cys38,

 

suggesting its role in initiating the oxidation that leads to the formation of the NOS bridge.[182]

The NOS bridge distinguishes itself from other protein-derived cofactors by its reversibility, enabling it to function as an allosteric redox switch. Under oxidizing conditions, the formation of the NOS bridge disrupts enzymatic activity, whereas reducing conditions restore the enzyme's functionality by breaking the crosslink. This reversible mechanism provides an elegant means of modulating enzyme activity in response to cellular redox states.

Computational studies shed light on the plausible mechanism of NOS bridge formation. The favored pathway involves the oxidation of the cysteine thiol by reactive oxygen species (ROS) to generate sulfenic acid, while the lysine amine undergoes oxidation to form hydroxylamine or an amine oxide.[214] A condensation reaction between sulfenic acid and hydroxylamine, accompanied by water elimination, results in the formation of the NOS bridge. This mechanism not only highlights the versatility of oxidative modifications in enzyme regulation but also adds to the growing repertoire of protein-derived cofactors with unique functional and structural properties. Similarly, cysteinesulfenic acid, Cys-(*S*)-OH, and derivatives stabilized by elements of protein structure as novel protein cofactors in enzyme catalysis and redox regulation have been appreciated.[17,33–35]

### 3.5. Cys–Tyr crosslinks

Cys–Tyr crosslinks are versatile protein-derived cofactors that differ in their functional roles depending on their structural context. While radical-containing Cys–Tyr cofactors are directly involved in catalysis as the catalytic driving force to provide an oxidizing equivalent to the bound substrate (Fig. 1, **29**), radical-free Cys–Tyr crosslinks (Fig. 1, **28**) often serve to amplify catalytic efficiency.[12,215] These crosslinks are integral to the activity of a range of enzymes, including thiol dioxygenases and reductases, underscoring their importance in diverse biochemical processes.

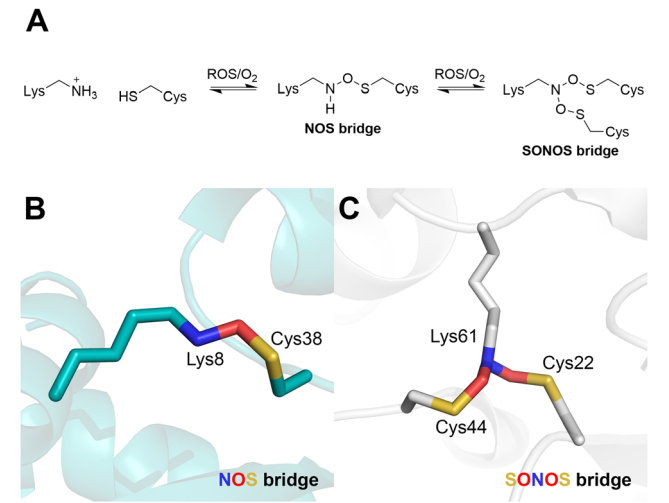


Fig. 11 (A) General cofactor biogenesis mechanism of NOS/SONOS bridge.[213] Crystal structures of NOS/SONOS redox switches. (B) Oxidized *Ng*TAL, showing the NOS bridge formed by the crosslink of Lys8 and Cys38 (turquoise; PDB 6ZX4). (C) $M^{pro}$ of SARS-CoV-2 in complex with inhibitor MPI8, possessing a SONOS bridge formed by the crosslink of Cys44, Lys61, and Cys22 (gray; PDB 7UUA).

**3.5.1. Cys–Tyr in thiol dioxygenases: catalytic amplification in thiol metabolism and oxygen sensing.** Cysteine dioxygenase (CDO) and cysteamine dioxygenase (ADO) are the only known mammalian thiol dioxygenases. They utilize a mononuclear nonheme iron center to catalyze oxygen insertion into sulfur-containing substrates. CDO converts L-cysteine to cysteine sulfinic acid, playing a crucial role in thiol metabolism and redox homeostasis. Similarly, ADO catalyzes the dioxygenation of cysteamine and *N*-terminal cysteine-containing proteins, such as regulators of G-protein signaling (RGS4 and RGS5) in the *N*-degron pathway and interleukin-32.[216–220] Thus, these enzymes play critical roles in thiol metabolism and redox regulations.[221,222]

The Cys–Tyr crosslink was first observed in the mouse CDO crystal structure,[188] and later in rat and human CDO structures (Fig. 12A).[14,223] This crosslink is not essential for catalysis but enhances catalytic efficiency by approximately 20-fold. Initially, Tyr157 was believed to initiate cofactor formation;[224] however, recent structural and computational studies indicate that Cys93 undergoes the initial oxidation.[14,225] The protein-derived cofactor is "untouchable" by traditional site-directed mutagenesis, as such mutations disable cofactor synthesis.

By introducing non-proteinogenic unnatural amino acids to specifically substitute the cofactor-bearing residues through genetic code expansion, the Cys–Tyr crosslink mechanism in human CDO has become better understood.[14,225] Subsequent studies in human ADO[12] and galactose oxidase[13] have contributed to this understanding and showcased that this non-canonical amino acid substitution is a powerful approach to studying protein-derived crosslink cofactors. The ternary complex structure of a genetically modified variant with 3,5-difluoro-L-tyrosine 157 ($F_2$-Tyr157) CDO bound to substrate cysteine and an $O_2$ structural surrogate nitric oxide ($^{\bullet}$NO) at 1.96 Å resolution revealed that $^{\bullet}$NO is equidistant (3.1 Å) from both Cys93 and Tyr157 residues, with $F_2$-Tyr157 additionally hydrogen-bonded to the substrate's carboxyl group.[225] This interaction suggests that Cys93 is the preferred site of initial oxidation.[14,225]

Mechanistically, substrate binding to the ferrous iron center generates an iron-bound superoxide radical, which oxidizes Cys93 to produce a thiyl radical. Tyr157 is subsequently oxidized by this thiyl radical, forming the Cys–Tyr crosslink (Fig. 13).[225] CDO plays a central role in thiol metabolism with its substrate level fluctuating in cells in a large range depending on the metabolic states of fed, fasting, and starvation, it is proposed that the Cys–Tyr cofactor is formed after hundreds of turnovers to amplify the catalytic efficiency in the presence of excess substrate.[226] This cofactor formation was first reported in 2006, establishing CDO as a model system for studying thiol dioxygenases.

In 2018, ADO was discovered to harbor a Cys–Tyr cofactor through mass spectrometry and $^{19}$F-NMR spectroscopy,

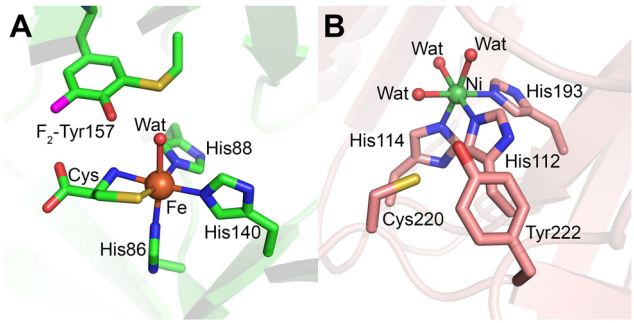


Fig. 12 Cys–Tyr cofactor in mammalian thiol dioxygenases. (A) Cysteine-bound $F_2$-Tyr157 hCDO (lime green; PDB 6BPV). (B) Cofactor-free Ni-ADO (salmon; PDB 7REI) is hexa-coordinated by three histidine residues, and three water molecules. Cofactor formation requires iron, cysteamine, and molecular oxygen therefore the crosslink is not expected in the Ni-bound crystal structure, but the crosslink has been detected *via* mass-spec in previous work.

representing a variation of this motif (Fig. 12B).[12] Unlike CDO, ADO's cofactor residues, Cys220 and Tyr222, are located adjacent to each other in the protein sequence, allowing the crosslink to form without inducing significant structural changes. This proximity confers structural flexibility, enabling ADO to accept substrates of varying sizes, from small thiol metabolites like cysteamine to larger *N*-cysteine peptides. The presence of the Cys220-Tyr222 crosslink increases the catalytic rate of ADO by more than 10-fold[12] through a concerted dioxygen transfer mechanism.[227]

Importantly, ADO exhibits dual functionality in thiol metabolism and oxygen sensing, leveraging its Cys–Tyr cofactor for catalytic enhancement only in thiol metabolism. The cofactor is not needed for oxygen sensing. Since the oxygenation of large protein substrates does not require a catalytic rate boost as cysteamine does during various metabolic states, the Cys–Tyr cofactor is not always synthesized in ADO.[217,219] Additionally, Cys220 and Tyr222 sit in a dynamic loop that likely moves away from the catalytic iron center when the target residue of a protein substrate arrives.[217] This trait makes the Cys–Tyr crosslink less frequently encountered in ADO and challenging to observe. It has been detected by protein mass spectrometry for the wild-type enzyme and shows approximately 50% occupancy for crosslinked and uncrosslinked forms in the $F_2$-Tyr222 human ADO variant.[12] Like LTQ,[211] a crystal or cryo-EM structure of ADO with a mature Cys–Tyr cofactor remains unavailable to date, even though its uncrosslinked cofactorless structure is available for both human[217] and mouse[218] ADO proteins.

**3.5.2 Cys–Tyr in reductive and nitrosative stress responses.** Beyond thiol dioxygenases, Cys–Tyr crosslinks have been identified in sulfite reductase, cytochrome *c* nitrite reductase, and putative zinc protease BF4112.[15,16] These enzymes exemplify the broader functional spectrum of Cys–Tyr crosslinks, from catalytic amplification to electron transfer and structural stabilization. In sulfite reductase, the Cys–Tyr crosslink stabilizes the enzyme's active site, facilitating electron transfer during the reduction of sulfite to hydrogen sulfide. Similarly, cytochrome *c* nitrite reductase utilizes this crosslink for nitrite reduction under nitrosative stress, showcasing the adaptability of this cofactor across diverse reaction mechanisms.

The unique properties of Cys–Tyr crosslinks, particularly their ability to amplify enzymatic efficiency and stabilize catalytic intermediates, make them a recurring motif in enzyme

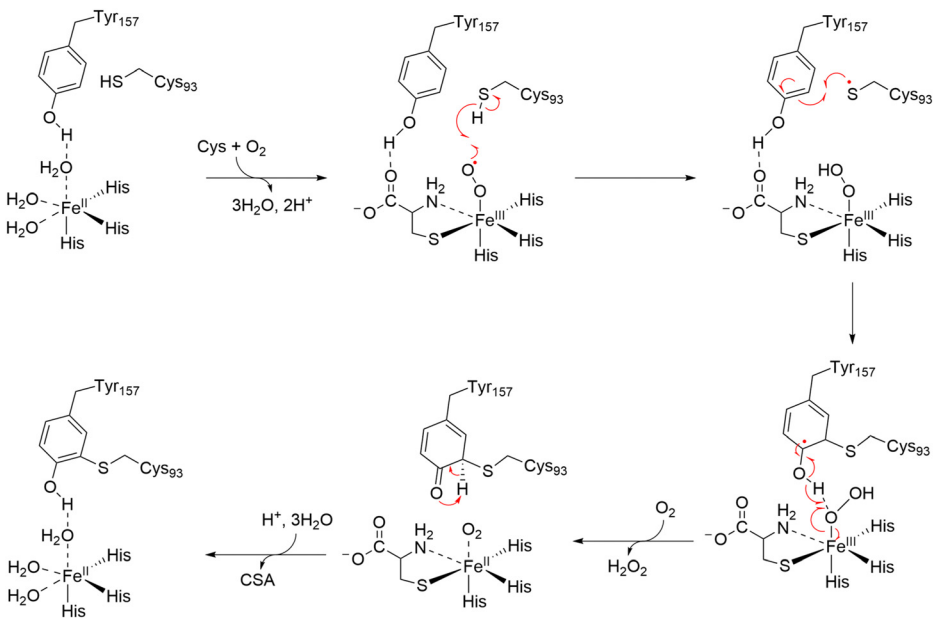


Fig. 13 Proposed mechanism of formation of Cys–Tyr crosslink in CDO.[225] Upon substrate binding to the Fe(II) center, an iron-bound superoxide radical is generated. The radical oxidizes Cys93, forming a thiyl radical and iron-bound hydroperoxide. The thiyl radical oxidizes Tyr157, generating the Cys–Tyr crosslink, and a transient-state radical species in Tyr157. C–H bond cleavage is driven by the formation of a ketone species after deprotonation of the hydroxyl group in the iron-bound hydroperoxide.

 

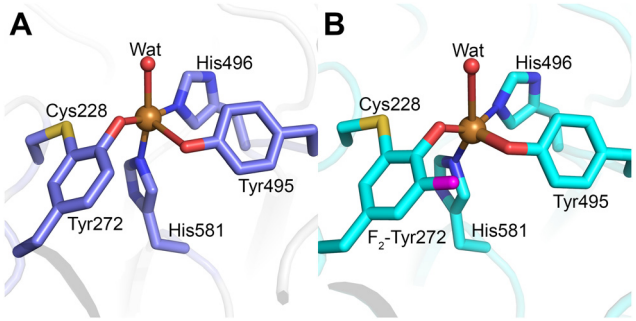


Fig. 14 Active sites of GAO and $F_2$-Tyr272 GAO showing the (Cys–Tyr)• cofactor. (A) Active site of GAO (purple; PDB 6XLT) shows the crosslink between Tyr272 and Cys228, with the copper ion coordinated in square pyramidal geometry by two histidines, Tyr495, and cofactor-bearing Tyr272. (B) Active site of $F_2$-Tyr272 GAO (teal; PDB 6XLS) retaining a monofluorinated (Cys–Tyr)• cofactor through the oxidative C–F bond cleavage during autocatalytic cofactor formation.[13]

evolution. Continued exploration of these crosslinks promises to uncover new insights into their functional roles and mechanistic diversity in biological systems.

### 3.6. Stable (Cys–Tyr)• cofactor in copper-radical oxidases

The (Cys–Tyr)• cofactor represents a remarkable example of a stable yet catalytically potent crosslinked radical cofactor distinct from those derived from a single amino acid such as glycyl or tyrosyl radicals in RNR and PS II. It is a copper ligand in a superfamily of copper-radical oxidases oxidizing a variety of diverse carbohydrates.[228,229] Permanently stabilized within the enzyme's active site, this tyrosyl radical (Tyr•),[186,230] covalently linked to a cysteine residue *via* a thioether bond,[2,187] is akin to the tyrosyl radical in RNR. However, its reactivity is finely tuned to serve as the catalytic driving force for the specific substrates of its host enzyme. This duality of stability and reactivity distinguishes the (Cys–Tyr)• cofactor from the radical-free Cys–Tyr crosslinks discussed earlier.

In copper-dependent galactose oxidase (GAO), the (Cys–Tyr)• cofactor is central to the enzyme's ability to catalyze the two-electron oxidation of a wide range of primary alcohols to their corresponding aldehydes, coupled with the reduction of molecular oxygen to hydrogen peroxide.[2,229,231–233] This reaction is facilitated by the synergy between the (Cys–Tyr)• radical and the Cu(II) ion, a unique coupling that enables two-electron redox chemistry with a single copper center.[229,231,233,234] The (Cys–Tyr)• radical is a metal ligand and permanently stabilized through antiferromagnetic coupling with the Cu(II) ion, making it EPR-silent, as confirmed by Whittaker and Whittaker using X-ray absorption near-edge spectroscopy (XANES).[230,235] The antiferromagnetic coupling renders both paramagnetic centers, Cu(II), and the (Cys–Tyr)• ligand, spectroscopically silent in EPR experiments. However, the hidden Cu(II) center becomes EPR-active when the (Cys–Tyr)• radical is neutralized by a radical scavenger, hydroxyurea, and hidden again upon one-electron oxidation by $K_3Fe(CN)_6$.[13]

The radical cofactor is formed by the covalent linkage of Cys228 and Tyr272 through an autocatalytic, irreversible post-translational modification.[229,231] The crystal structure of GAO revealed that the sulfur atom of Cys228 forms a thioether bond with the $C_\varepsilon$ of Tyr272, a crosslink essential for catalytic function.[187] This configuration supports the radical's stability while allowing it to participate in substrate oxidation.

Mutagenesis studies have reinforced the importance of the cofactor. Substitution of Cys228 with glycine (C228G) abolished cofactor formation and reduced catalytic efficiency by approximately 1000-fold, underscoring the critical role of the sulfur atom in stabilizing the Tyr• radical.[236,237] Synthetic model studies have provided additional mechanistic insights, demonstrating that thioether substitutions lower the phenol's p$K_a$ and reduction potential, facilitating radical formation and stabilization.[234]

Recent advances in genetic code expansion have offered new perspectives on the cofactor's properties and formation.[238] Substitution of Tyr272 with $F_2$-Tyr retained cofactor formation but reduced catalytic efficiency to 12% of the wild-type enzyme. Structural studies of $F_2$-Tyr GAO revealed the formation of a monofluorinated radical cofactor *via* C–F bond cleavage,

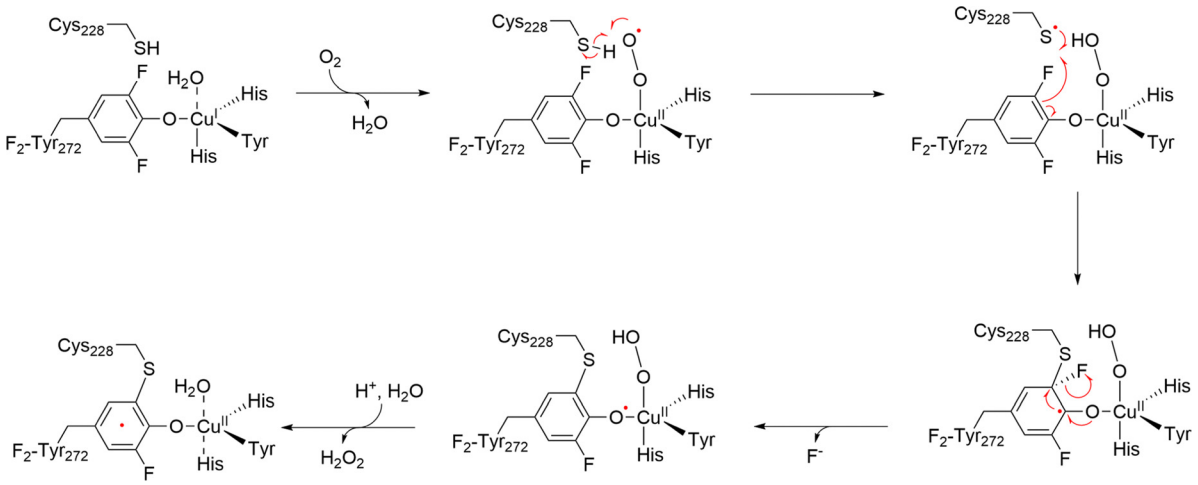


Fig. 15 Proposed biogenesis mechanism of the (Cys–Tyr)• in $F_2$-Tyr272 GAO.

illustrating how electronic modifications influence the radical's reactivity and stability (Fig. 14).[13,239]

The proposed cofactor maturation mechanism involves a copper-bound superoxide radical oxidizing the thiol group of Cys228, forming a copper-bound hydroperoxide intermediate and a thiyl radical. This thiyl radical then oxidizes Tyr272 (or $F_2$-Tyr272), resulting in the formation of the thioether bond and the mature (Cys–Tyr)$^\bullet$ cofactor (Fig. 15).[13,239]

In addition to GAO, the (Cys–Tyr)$^\bullet$ cofactor is found in glyoxal oxidase (GLOX) and other copper radical oxidases, where it drives diverse catalytic reactions tailored to their specific substrates.[228,229,231] Its evolutionary significance and versatility underscore its importance as a powerful and highly specialized catalytic tool in enzymatic chemistry.

# 4. Protein cofactors derived from covalent crosslink of three or more amino acids

This section highlights protein-derived cofactors formed by the covalent crosslinking of three or more distinct amino acid residues. These trimeric or more crosslinks represent some of the most complex and functionally diverse modifications found in nature. By enhancing catalytic efficiency, stabilizing active sites, and introducing novel functionalities, these cofactors play critical roles in the biochemical processes of their host proteins. To date, four distinct trimeric crosslinked cofactors have been identified: Cys–Lys–Cys, Gly–Ala–Ser, Met–Tyr–Trp, and Ser–Tyr–Gly (Table 3). Additionally, the redox PQQ cofactor (Fig. 1, **37**) is formed from five amino acid residues Glu–Val–Thr–Leu–Tyr with further posttranslational oxidations. Below, we examine their structure, function, and synthesis mechanisms.

## 4.1. Cys–Lys–Cys crosslink with a SONOS bridge

The Cys–Lys–Cys cofactor represents a fascinating chemical feature involving a sulfur–oxygen–nitrogen–oxygen–sulfur (SONOS) bridge (Fig. 1, **33**). Initially identified in the main protease ($M^{pro}$) of SARS-CoV-2, this structure has garnered significant attention due to its role in the pathogenesis and replication of the virus, making it a prime drug target in COVID-19 research.[213,240]

Crystal soaking experiments revealed Y-shaped crosslinks between Cys22, Cys44, and Lys61 in $M^{pro}$ (Fig. 11C). Computational studies suggest that the SONOS bridge forms through a series of oxidation reactions, likely mediated by reactive oxygen species (ROS).[214] A thio-(hydro)peroxy acid intermediate has been identified as a plausible precursor to both NOS and SONOS bridges, with homolytic dissociation leading to NOS formation. However, the exact pathway for SONOS formation remains under investigation.

The regulatory role of SONOS and NOS bridges in $M^{pro}$ exemplifies their functional versatility. The reversible formation and dissolution of these crosslinks appear to act as redox switches, modulating enzymatic activity in response to oxidative stress. Further structural and mechanistic studies are crucial for understanding the formation and potential therapeutic exploitation of these cofactors.

## 4.2. Ser–Tyr–Gly crosslink in green fluorescent protein

The Ser–Tyr–Gly crosslink forms the fluorescent chromophore at the core of green fluorescent protein (GFP), a widely used tool in molecular and cellular biology.[245] GFP's chromophore is generated by the autocatalytic cyclization and oxidation of the Ser65 (or Thr65), Tyr66, and Gly67 residues within a tightly folded β-barrel structure (Fig. 1, **34**).

Unlike many cofactors, the formation of GFP's chromophore is spontaneous and requires no external enzymes. However, molecular oxygen is essential, as is precise protein folding to orient the residues for cyclization. The resultant chromophore exhibits a unique conjugated structure that absorbs blue light and emits green fluorescence (Fig. 16).

Mechanistic parallels have been drawn between the GFP chromophore and the methylene imidazolone (MIO) cofactor in histidase enzymes,[246] suggesting a shared evolutionary origin (Fig. 1, **35**).[21] Despite extensive use, the detailed mechanism of GFP chromophore biosynthesis remains elusive. Ongoing studies aim to elucidate these pathways, which may enable the engineering of fluorescent proteins with novel properties.

Table 3 Cofactors derived from covalent crosslink of three or more amino acids

| Source | Cofactor | New chemical bonds formed | Representative enzyme | Biogenesis | Function | Ref. |
|---|---|---|---|---|---|---|
| Cys–Lys–Cys | SONOS bridge | S–O–N–O–S | Main protease | Autocatalytic | Allosteric redox switch | 213 and 240 |
| Gly–Ala–Ser | MIO | C–N | Histidase | Autocatalytic | Catalysis | 241 |
| | MIO | C–N | Phenylalanine ammonia lyase | Autocatalytic | Catalysis | 242 |
| | MIO | C–N | Tyrosine ammonia lyase | Autocatalytic | Catalysis | 243 |
| $Met^+$–Tyr–Trp | $M^+YW$ | C–C, C–S | Catalase-peroxidase (KatG) | Autocatalytic | Enable catalase activity | 244 |
| $Met^+$–Tyr–Trp–OOH | $M^+YW$–OOH | C–C, C–S, C–O | Catalase-peroxidase (KatG) | Autocatalytic | Modulates catalase-peroxidase functions | 244 |
| Ser–Tyr–Gly | Ser–Tyr–Gly | C–N | Green fluorescent protein | Autocatalytic | Fluorescence emission | 245 |
| Glu–Val–Thr–Leu–Tyr | PQQ | C–C<br>C–N<br>C═O | Alcohol dehydrogenase, aminoadipic 6-semialdehyde dehydrogenase | Enzymatic: PqqE, PqqD, PqqF, PqqB, and PqqC | Catalysis | 203–205 |

 

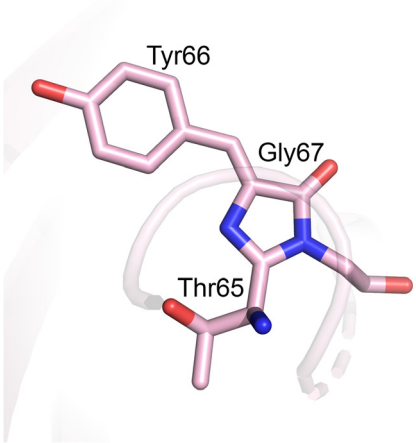


Fig. 16 Crystal structure of GFP cofactor formed by the cyclization and oxidation of Thr65, Tyr66, and Gly67 (pink; PDB 1EMA).

### 4.3. $Met^{+}$–Tyr–Trp cofactor in catalase-peroxidase

In the catalase-peroxidase enzyme (KatG), the $Met^{+}$–Tyr–Trp (MYW) cofactor is a trimeric crosslink critical for its bifunctional activity. KatG is a well-known enzyme, largely due to *Mycobacterium tuberculosis* KatG is an essential utility for activating the frontline antitubercular prodrug isoniazid (INH) and detoxifying reactive oxygen species such as $H_2O_2$, contributing to the pathogen's survival and virulence.[247] This bifunctional enzyme has emerged as a promising target in tuberculosis drug development, with chemical modification of the MYW cofactor rendering the bacterium more susceptible to peroxide-mediated immune clearance and simultaneously enhancing peroxidase activity to improve INH activation.[248]

The MYW cofactor, first characterized in *Haloarcula marismortui* KatG by X-crystallography, is autocatalytically formed during protein maturation.[249] Spectroscopic studies suggest that an Fe(IV)=O porphyrin cation radical oxidizes Met, Tyr, and Trp residues to generate the crosslinked structure.[250,251] This cofactor endows KatG with an exceptional single-function catalase-like activity, synergistically enhancing $H_2O_2$ detoxification by several orders of magnitude while retaining its innate peroxidase functionality.[251,252]

It has been proven through EPR coupled with isotope labeling that MYW becomes a transient MYW$^{\bullet}$ free radical after $H_2O_2$ binds to the adjacent heme and becomes activated, and a cofactor radical-based catalase mechanism is thus proposed.[253] The MYW cofactor spares one of the oxidizing equivalents and located next to the Fe(IV)=O, enabling strong coupling for $2e^{-}$ oxidation chemistry against subsequent $H_2O_2$ for catalase activity. Otherwise, the oxidizing equivalents from $H_2O_2$ are directed outside the heme center of KatG *via* aromatic residues to support $1e^{-}$ oxidation of organic substrates (*i.e.*, peroxidase activity).[252]

Interestingly, two forms of the MYW cofactor exist in nature: MYW (catalase-active) and MYW-OOH (catalase-inhibitory) (Fig. 1, **36a** and **36b**).[254–256] Studies of the solution state of as-isolated *M. tuberculosis* KatG indicate that the MYW-OOH cofactor can act as a molecular switch, toggling between active MYW and inactive MYW-OOH states depending on its environment conditions for the chemical structure of the trimeric cofactor, such as temperature and hydrogen peroxide levels.[254] This dual functionality underscores the evolutionary significance of the MYW cofactor in balancing oxidative defense and metabolic processes.

### 4.4. Pyrroloquinoline quinone (PQQ) cofactor in dehydrogenases

The crosslinked protein cofactor PQQ (Fig. 1, **37**) found in alcohol dehydrogenases and aminoadipic 6-semialdehyde dehydrogenase,[203–205] possesses two remarkably unique features. First, it is the only known protein cofactor derived from more than three amino acid residues. Second, it is the only one that does not remain covalently bound to the parent protein. The synthesis of PQQ starts from a tyrosine residue and subsequently involves crosslinking and further chemical modifications of glutamate, valine, threonine, and leucine residues (Fig. 17).[67,257] This complex process is facilitated by a series of auxiliary proteins: PqqE, PqqD, PqqF, PqqB, and PqqC. During the post-translational modifications (PTMs), this quinone cofactor loses the peptide connection but remains bound at the active site of the protein.[203]

## 5. Covalent crosslinks between heme and protein residues in metalloenzymes

Covalent linkages between heme and protein residues play crucial roles in the function and stability of heme-dependent enzymes. One well-known example is heme *c*, which is always covalently attached to two cysteine (Cys) residues of the associated protein. Its attachment occurs through thioether bonds formed between the vinyl side chains of the heme and the cysteine residues in the protein, creating a protein cofactor with the structure Cys–heme–Cys, which could be #38 if it were included in Fig. 1. While electron transfer is the primary function, heme *c* also plays other roles, such as in apoptosis and serving as a catalytic site in some enzymes. Due to its prevalence, heme *c* is not typically included in the protein-derived cofactor category.

These crosslinks, formed between heme substituents (such as vinyl groups) and amino acid side chains (like cysteine or histidine), can significantly impact catalysis and heme retention. In addition to heme *c*, a recent discovery shows that SfmD, a monooxygenase involved in saframycin A biosynthesis, contains a mono-covalently linked Cys–Heme.[36] SfmD possesses an autocatalytically generated thioether crosslink between the heme 4-vinyl group and Cys317 (Fig. 1, **17**). This covalent bond is essential for catalytic activity, as demonstrated by the complete loss of activity upon mutation of Cys317 to serine or alanine. The observation of Cys–heme in the crystal structure of an oxygenase in SfmD is surprising, as all other characterized members of the same superfamily, known as heme-dependent aromatic oxygenase (HDAO), contain a heme *b* without

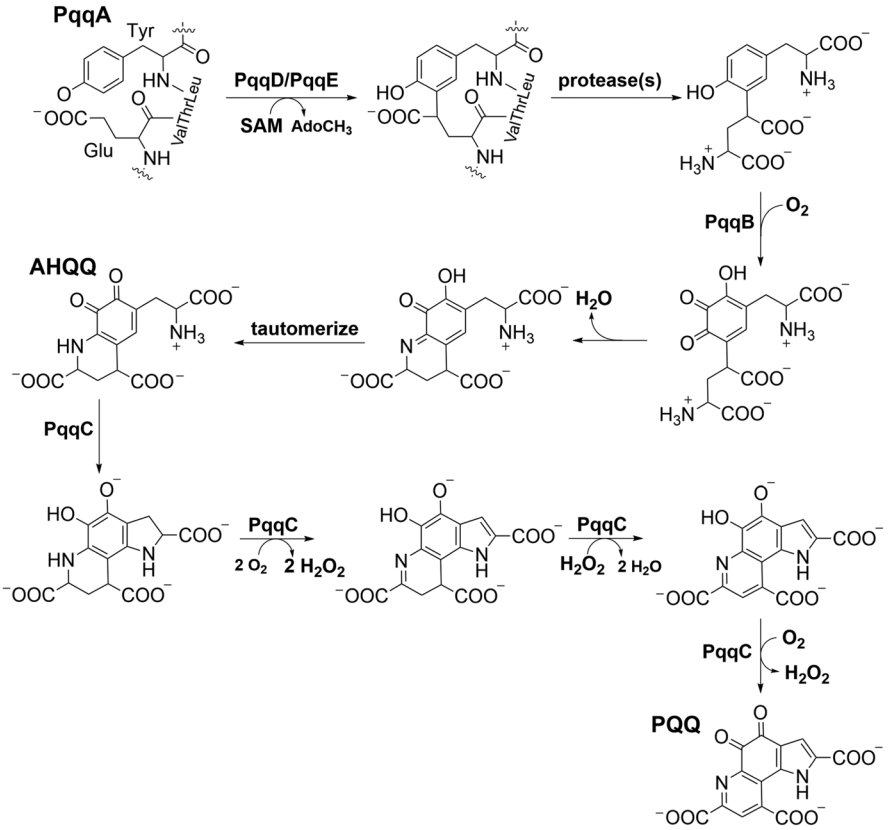


Fig. 17 Enzymatic synthesis PQQ consists of nine steps including crosslink and chemical modifications of five amino acid residues.[67]

crosslink and thioether bond attachment.[258] This unique linkage enables dynamic rotation of the heme plane during substrate binding while maintaining heme retention at the active site. Such substantial heme center dynamics are warranted in this enzyme, as the heme has two axial histidine ligands; one of these dissociates during catalysis upon substrate binding and then re-coordinates to the heme iron at the end of the catalytic cycle (Fig. 18A). This dynamic coordination adds a significant trigger for enhancing the oxidation power of the heme. Given that this enzyme can also utilize L-Tyr as an alternative substrate, albeit with lower efficiency compared to its native substrate, 3-methyl-L-Tyr, this unusual heme cofactor with a single covalent crosslink to a cysteine residue and an additional mobile distal histidine ligand may be crucial for preventing misfire and L-Tyr depletion.

The formation of this Cys–heme crosslink has been partially replicated in sperm whale myoglobin by introducing a cysteine residue near the heme 4-vinyl group under reducing conditions, further validating the feasibility of this type of modification.[261] Another distinct type of covalent heme-protein crosslink involves a histidine residue and the heme group. This unprecedented histidine-heme bond was discovered in hemoglobins from the cyanobacteria *Synechocystis* sp. PCC 6803 and *Synechococcus* sp. PCC 7002 (GlbN). In these proteins, the crosslink forms between the heme 2-vinyl group and a histidine residue (Fig. 1, **18**). Site-directed mutagenesis and NMR studies have confirmed the functional role of this crosslink, particularly in catalysis.[44,260] This discovery has spurred research into exploiting this type of linkage for protein engineering. Introducing a histidine residue near a heme vinyl group has been shown to improve heme retention. This strategy has been successfully applied to myoglobin and *Chlamydomonas* hemoglobin by mimicking the crosslink observed in cyanobacteria.[262,263] Reminiscent of SfmD, GlbN also has a *bis*-His coordination with the heme and shows oxygenation activity. GlbN is capable of •NO dioxygenase activity, where the His–heme crosslink enables •NO reduction to HNO.[264] The proposed biogenesis mechanism of this modification involves the nucleophilic attack of a neutral histidine residue to a $C_\alpha$ carbocation (Fig. 18B).[260]

## 6. Modern approaches revitalize crosslinked cofactor studies

While the discovery of protein-derived crosslinked cofactors initially sparked significant interest, the field has experienced limited progress in the past two decades. The inherent, irreversible nature of these crosslinks, forming only once per protein molecule, renders traditional mutagenesis approaches ineffective. This ''untouchable'' characteristic, coupled with the frequent absence of spectroscopic signatures, has hindered studies of their biogenesis and catalytic roles. Relying solely on mass spectrometry or structural determination for crosslink

 

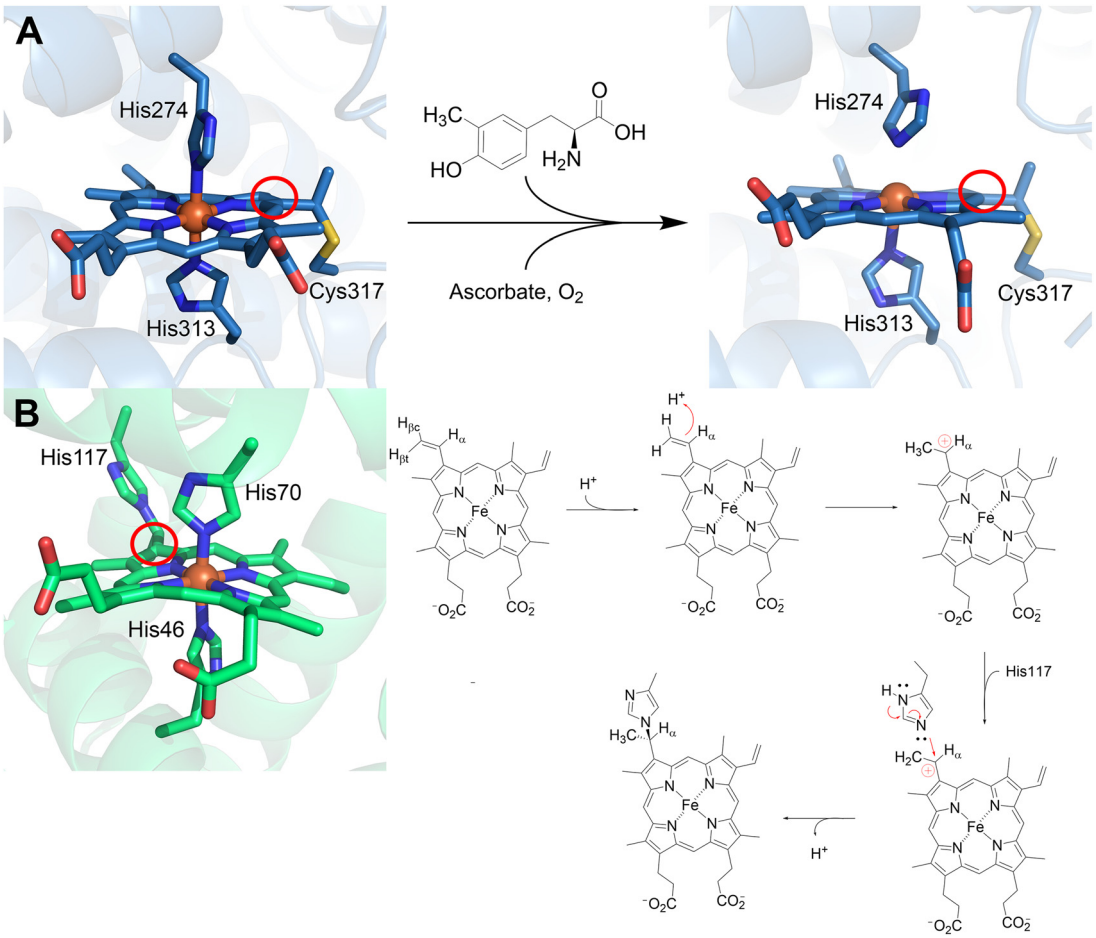


Fig. 18 Crosslinks to heme moieties in SfmD and GlbN. (A) SfmD has a unique Cys–heme crosslink at the 4-vinyl group used for catalysis, two conformations are shown. Initially, there is *bis*-His coordination and presence of the crosslink (left, navy blue; PDB 6VDQ), upon addition of 3-Me-L-Tyr, ascorbate, and oxygen, His274 disassociates (right, navy blue; PDB 6VE0).[36] (B) GlbN has a His–heme crosslink at the 2-vinyl group also used for catalysis. Like SfmD, it presents *bis*-His coordination (left, green; PDB 4MAX).[259] The right side shows the proposed biogenesis mechanism of the His–heme crosslink in GlbN where the 2-vinyl group is protonated at the $C_\beta$ position to yield a $C_\alpha$ carbocation. The carbocation then undergoes a nucleophilic attack by His117, producing the mature crosslink.[260]

detection is impractical for routine analyses. Moreover, the stochastic, post-catalytic formation of these cofactors, occurring after an undefined number of catalytic cycles, further complicates mechanistic investigations. Consequently, the field has stagnated, demanding new strategies to unlock the secrets of crosslinked cofactor synthesis and function.

Recently, an innovative approach employing site-specific non-canonical amino acid (ncAA) substitution has emerged as a powerful tool for reviving the crosslink cofactor field.[12,14] By replacing cofactor-bearing residues with ncAAs, such as unnatural amino acid 3,5-difluoro-L-tyrosine, or L-3,4-dihydroxyphenylalanine (L-DOPA) from over 500 naturally occurring amino acids, the studies can maintain the essential chemical character of the target while introducing specific functional modifications. This method bypasses the limitations imposed by the irreversible crosslinks.

The ncAA-incorporation and site-specific cofactor substitution is an innovative, viable and rigorous approach to gain new insights into cofactor assembly and the catalytic properties of an enzyme. The ncAA incorporation strategy utilizes engineered tRNA/aminoacyl-tRNA-synthetase (aaRS) pairs and amber codon suppression to introduce desired amino acids during translation. The development of robust pEVOL vectors and commercially available ncAA systems has significantly enhanced this technology. This method consists of: (1) a plasmid that expresses aaRS pair which has been evolved to incorporate a specific ncAA, and (2) a plasmid of the gene of interest with a modified codon at the desired site (usually substituted with an amber stop codon) that will be recognized by the cognate charged tRNA (Fig. 19). This method allows for the ncAA to be incorporated using native protein translation machinery. After years of resilient research, the pEVOL vector was developed to enhance non-canonical amino acid incorporation in *E. coli*, with at least 34 plasmids coding for different ncAAs commercially available.[265]

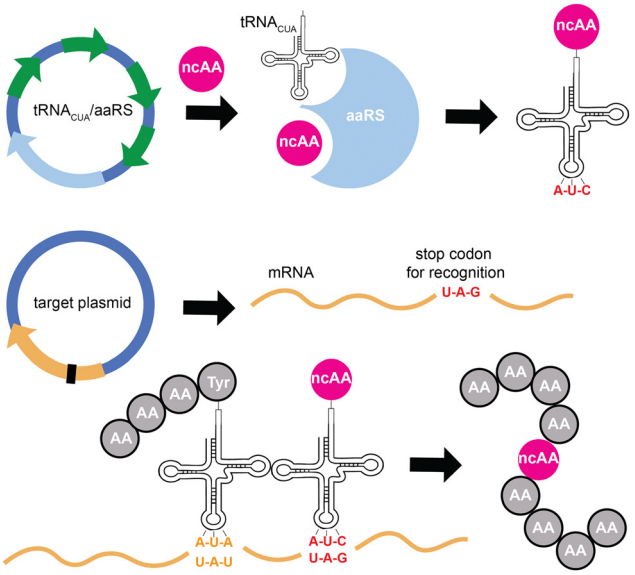


Fig. 19 Cartoon diagram of genetic incorporation of non-canonical amino acids into proteins.

Protein-derived cofactor studies greatly benefit from the ongoing development of aaRS/tRNA$_{CUA}$ pairs that expand the toolbox to accurately and precisely probe mechanisms of formation, kinetics, and structural changes. Applications in bacterial RNR,[266,267] thiol dioxygenases (CDO/ADO),[12,14,225] and oxidases (GAO).[13,238] These studies provided experimental evidence to support a new Cys–Tyr crosslink in ADO, direct evidence for the involvement of two tyrosine residues in radical propagation in RNR I, and evidence to support a concerted O–O transfer instead of a stepwise O-atom transfer proposed for CDO catalytic pathway, *etc.*

Continued development and expansion of ncAA incorporation techniques will be crucial for advancing our understanding of protein-derived cofactors. This approach offers a promising avenue for capturing catalytic intermediates, enabling novel reactions, and enhancing existing functions in a broad range of biological systems beyond those harboring crosslinked cofactors.[268]

## 7. Bridging synthetic applications and mechanistic understanding

Many of the protein-derived cofactors discussed are essential for catalytic activity, either directly or indirectly. This opens two major avenues of discovery: (1) synthesizing mechanistic probes to challenge a system and gain a mechanistic understanding of the cofactors for their role in catalysis, and (2) synthesizing inhibitors to prevent the formation of essential cofactors in undesired systems. Moreover, using synthetic models, either directly or through incorporation with proteins, has garnered attention, such as in the efforts led by Hayashi and colleagues.[79,120,269–272]

### 7.1 Development of biomimetic systems

Quinones have applications in organic synthesis, catalysis, and industry due to their unique redox properties. They readily undergo reversible two-electron reductions, and their ability to present multiple oxidation states (quinone, semiquinone, and hydroquinone) allows for versatile reaction outcomes.[273] Quinones resembling those present in the cofactors of CuAOs and other quinoproteins have been generated to investigate quinone-catalyzed oxidations of organic substrates and compare them to quinones with high reduction potentials.[274] Using PQQ as a model, phenanthroline-derived quinones were synthesized and challenged with primary and secondary amines. The reaction products supported the hypothesis of a transamination mechanism.[275] This mechanistic study focused on exploring how quinone moieties are reduced by their substrates. The quinones available in biological systems that operate at ambient conditions serve as a window to investigate how other naturally occurring quinones catalyze their designated reactions. These quinones are commonly seen in fungicides, allelochemicals, and siderophores.[273]

Functional models of the SCS Ni(II) pincer complex found in LarA, also called the NPN cofactor, have been generated to study the cofactor's role in the catalytic mechanism.[276–278] One of the previous models for the NPN cofactor contained thioamide groups at the C2 and C3 positions, and catalyzed alcohol dehydrogenation irreversibly with no racemization, opposite of the canonic mechanism of LarA.[276] A further optimized model which replaced the thioamide groups with thiocarboxylates is more structurally similar to the NPN cofactor and displayed lactate racemization, serving as a better-suited mechanistic probe.[277] Combined computational and experimental studies highlight two possible pathways, but the more favorable one involves the reversible proton-coupled hydride transfer to C1 of the NPN cofactor.[277] These studies demonstrate the importance of using protein-derived cofactors as model systems when designing new metal-based catalysts and/or pincer ligands, in this case, for alcohol dehydrogenation reactions.[276]

GAO is a well-rounded enzyme that has gained a lot of attention due to its ability for C–H and, recently found, C–F bond functionalization under ambient conditions.[13] A substantial amount of work has been done to generate GAO model compounds that are capable of C–sp$^3$–H oxidations with equal or greater activity/selectivity.[234,279–283] Many of these GAO biomimetic systems attempt to mimic the enzyme active site or the tyrosyl radical to catalyze the same chemistry. These systems are also incorporated into the use of biosensors given that galactose quantification is highly relevant in the dairy/fermentation industries. Methods using GAO as a biosensor date back to 1977,[284] and continue to be optimized in the present day.[285]

### 7.2 Biocatalysis

Protein-derived cofactors have expanded the toolbox for enzymatic reactions, offering unique catalytic properties such as regio- and stereoselectivity. A prominent example is found in alcohol oxidation/dehydrogenation reactions. Copper-radical oxidases (CROs) such as galactose oxidase and glyoxal oxidases are a subset of enzymes that catalyze the two-electron oxidation of primary alcohols, concomitant with the reduction of molecular oxygen to hydrogen peroxide, without using external

 

organic cofactors since they have a built-in Cys–Tyr radical cofactor that aids in catalysis.[228] On the contrary, alcohol dehydrogenases (ADHs) and alcohol oxidases (AOXs) both require external cofactors that are either $NAD^+$-based or FAD-based for catalysis.[286] The broad substrate range accepted by CROs and their ability to only require molecular oxygen for catalysis has highlighted their potential applications as environmentally friendly biocatalysts for industrial, bioengineering, and biotechnological purposes.[287,288]

## 8. Structural variations and function diversity

Protein-derived cofactors are remarkable products of posttranslational modifications that transform mundane amino acid residues into unique catalytic or structural moieties. These cofactors introduce novel functions such as redox switching, catalytic rate/efficiency amplification, adding a new function or converting a precursor protein to a functionally active enzyme, vastly expanding the functional repertoire of proteins. Even cofactors derived from identical amino acids can display distinct functions based on their position and conformations within their host enzymes. The evolution of these cofactors reflects nature's ability to optimize proteins for increasingly complex biological roles.

A striking example of structural variation in a protein-derived cofactor is the two unique cofactor forms in KatG, MYW and MYW-OOH (Fig. 20). Previous crystallography studies identified an indole-*N*-linked hydroperoxyl group MYW-OOH cofactor, and recently this MYW-OOH form was extensively studied in solution and compared to the active MYW form.[254] The MYW-OOH cofactor was first identified in crystal structures of KatG expressed at 25 °C, while the MYW form predominates in KatG expressed at 37 °C. Resonance Raman (rR), electron paramagnetic resonance (EPR), mass spectrometry, and X-ray crystallographic studies confirmed the reversible interconversion between these forms.

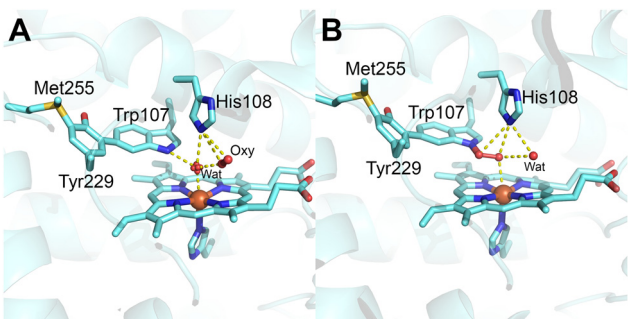


Fig. 20 Heme pocket of *M. tuberculosis* KatG with focus on MYW crosslink and His108, a catalytically relevant distal residue. (A) MYW form of KatG's cofactor that supports catalase activity (cyan; PDB 8W1X) shows a putative $O_2$ molecule, presumably a decomposed product of the hydroperoxyl moiety. (B) Natural MYW-OOH form of KatG's cofactor that presents limited catalase activity (cyan; PDB 8W1W).[254]

Structural variation is also evident in the Lys–Cys–NOS cofactor of *Neisseria gonorrhoeae* transaldolase (*Ng*TAL), which functions as a reversible redox switch. In its oxidized state, the cofactor contains a sulfur–oxygen–nitrogen–oxygen–sulfur (NOS) bridge, detectable *via* sulfur K-edge X-ray absorption spectroscopy (XAS).[289] Upon reduction, the NOS bridge is absent, and *Ng*TAL becomes catalytically active, reverting to inactivity over time as the oxidized form reforms. Unlike most protein-derived cofactors, which enhance catalytic efficiency, the NOS bridge decreases *Ng*TAL's catalytic activity. Computational studies indicate that the high-energy nature of the NOS bridge supports its reversibility, allowing the enzyme to cycle between active and inactive states. These features make the NOS cofactor an intriguing target for studies in protein engineering and drug discovery, particularly for applications requiring redox-controlled enzymatic switches.

The structural plasticity of protein-derived cofactors highlights their adaptability in response to environmental or cellular cues. Variations in cofactor structure often directly influence enzymatic activity, substrate specificity, or regulatory mechanisms, underscoring the evolutionary ingenuity of these modifications. As seen with the MYW and NOS cofactors, structural variants may serve as molecular switches, toggling between states to regulate biological functions dynamically.

## 9. Summary and perspective

This review has explored the fascinating world of amino acid modifications and crosslinking in proteins, emphasizing the structural and functional diversity of protein-derived cofactors and their transformative role in enzymology. Originating from PTMs, these cofactors reveal a hidden layer of protein complexity, enabling enzymes to perform functions that extend beyond the capabilities of unmodified amino acid residues. In particular, the amino acid residue crosslinking process isn't just about molecular intricacies—it's about the creation of novel redox centers that significantly impact enzyme functionality. This burgeoning field has unveiled a new level of protein complexity, as evidenced by the discovery of protein-derived cofactors. Since the foundational work of Okeley and van der Donk two decades ago, which summarized 17 distinct cofactors, the field has expanded significantly, now encompassing 38 unique types (42 when free radical forms are counted), categorized into three major groups: single amino acid-derived cofactors, two-residue crosslinked cofactors, and trimeric crosslinked cofactors.

A recurring theme in cofactor biogenesis is the involvement of metal centers. Protein-bound metals such as iron and copper often facilitate the complex chemical transformations necessary for cofactor formation, acting as catalytic mediators in autocatalytic or enzymatically driven pathways. While not all cofactors require metal centers, most characterized cases display the integral role of metalloproteins in enzymatic catalysis and the generation of protein-derived cofactors.

The discovery of these protein-derived cofactors underscores the versatility and ingenuity of nature's enzymatic toolbox. Beyond enhancing catalytic efficiency, protein-derived cofactors drive the evolution of novel biochemical pathways and regulatory mechanisms. Advances in structural biology, including X-ray crystallography, cryo-electron microscopy, and emerging biophysical techniques, have been instrumental in identifying and characterizing these cofactors, paving the way for future discoveries.

Despite these advances, significant challenges remain. The lack of predictive methods for identifying PTMs and the limited understanding of cofactor formation pathways highlight the need for further research. Protein-derived cofactors remain the most challenging aspect of protein structure–function relationships, for even the most advanced AI models. Research advances in this area will help generative AI grow stronger and more accurate in predicting protein structure and functions. Further studies will connect and integrate bioinformatics, structural biology, and metalloenzyme chemistry to elucidate the rules governing cofactor formation and function.

It is important to note that twenty-two genetically coded amino acids aren't enough for catalysis. At least 38 protein-derived cofactors play critical roles in enhancing or even introducing new catalytic activities in enzymes. As the field progresses, the study of protein-derived cofactors promises to yield new insights into enzymology, protein evolution, novel catalytic functions, and bioengineering. These insights will deepen our understanding of fundamental biological processes, and offer innovative strategies for applications in biotechnology, drug discovery, and synthetic biology.

## Data availability

All data supporting this study are included in the manuscript. All figures are original, created by the authors, and appropriately cited where external sources were used to support their illustrations.

## Conflicts of interest

There are no conflicts to declare.

## Acknowledgements

This work was supported by the National Institutes of Health (NIH) under award numbers GM108988 and GM152982, the National Science Foundation (NSF) award under CHE-2204225, and the Welch Foundation grant AX-2110-20220331. A. L. acknowledges the generous support of the Lutcher Brown Endowment Fund.

## References

1 L. Xie and W. A. Van der Donk, *Proc. Natl. Acad. Sci. U. S. A.*, 2001, **98**, 12863–12865.
2 N. Ito, *Seibutsu Butsuri*, 1992, **32**, 300–305.
3 M. D. Swain and D. E. Benson, *Proteins*, 2005, **59**, 64–71.
4 V. L. Davidson, *Biochemistry*, 2007, **46**, 5283–5292.
5 J. Abramson, J. Adler, J. Dunger, R. Evans, T. Green, A. Pritzel, O. Ronneberger, L. Willmore, A. J. Ballard, J. Bambrick, S. W. Bodenstein, D. A. Evans, C.-C. Hung, M. O'Neill, D. Reiman, K. Tunyasuvunakool, Z. Wu, A. Žemgulytė, E. Arvaniti, C. Beattie, O. Bertolli, A. Bridgland, A. Cherepanov, M. Congreve, A. I. Cowen-Rivers, A. Cowie, M. Figurnov, F. B. Fuchs, H. Gladman, R. Jain, Y. A. Khan, C. M. R. Low, K. Perlin, A. Potapenko, P. Savy, S. Singh, A. Stecula, A. Thillaisundaram, C. Tong, S. Yakneen, E. D. Zhong, M. Zielinski, A. Žídek, V. Bapst, P. Kohli, M. Jaderberg, D. Hassabis and J. M. Jumper, *Nature*, 2024, **630**, 493–500.
6 M. Baek, F. DiMaio, I. Anishchenko, J. Dauparas, S. Ovchinnikov, G. R. Lee, J. Wang, Q. Cong, L. N. Kinch, R. D. Schaeffer, C. Millán, H. Park, C. Adams, C. R. Glassman, A. DeGiovanni, J. H. Pereira, A. V. Rodrigues, A. A. van Dijk, A. C. Ebrecht, D. J. Opperman, T. Sagmeister, C. Buhlheller, T. Pavkov-Keller, M. K. Rathinaswamy, U. Dalwadi, C. K. Yip, J. E. Burke, K. C. Garcia, N. V. Grishin, P. D. Adams, R. J. Read and D. Baker, *Science*, 2021, **373**, 871–876.
7 D. Chakravarty, M. Lee and L. L. Porter, *Curr. Opin. Struct. Biol.*, 2025, **90**, 102973(1–7).
8 T. C. Terwilliger, D. Liebschner, T. I. Croll, C. J. Williams, A. J. McCoy, B. K. Poon, P. V. Afonine, R. D. Oeffner, J. S. Richardson, R. J. Read and P. D. Adams, *Nat. Methods*, 2024, **21**, 110–116.
9 H. Longin, N. Broeckaert, V. van Noort, R. Lavigne and H. Hendrix, *Curr. Opin. Microbiol.*, 2024, **77**, 102425(1-7).
10 O. Carugo, *Comput. Biol. Chem.*, 2024, **110**, 108069(1-6).
11 W. Wang, Z. Gong and W. A. Hendrickson, *Acta Crystallogr., Sect. D:Struct. Biol.*, 2025, **81**, 4–21.
12 Y. Wang, W. P. Griffith, J. Li, T. Koto, D. J. Wherritt, E. Fritz and A. Liu, *Angew. Chem., Int. Ed.*, 2018, **57**, 8149–8153.
13 J. Li, I. Davis, W. P. Griffith and A. Liu, *J. Am. Chem. Soc.*, 2020, **142**, 18753–18757.
14 J. Li, W. P. Griffith, I. Davis, I. Shin, J. Wang, F. Li, Y. Wang, D. J. Wherritt and A. Liu, *Nat. Chem. Biol.*, 2018, **14**, 853–860.
15 S. E. Hromada, A. M. Hilbrands, E. M. Wolf, J. L. Ross, T. R. Hegg, A. G. Roth, M. T. Hollowell, C. E. Anderson and D. E. Benson, *J. Inorg. Biochem.*, 2017, **176**, 168–174.
16 R. J. Martinie, P. I. Godakumbura, E. G. Porter, A. Divakaran, B. J. Burkhart, J. T. Wertz and D. E. Benson, *Metallomics*, 2012, **4**(1037–1042), 1008.
17 A. Claiborne, T. C. Mallett, J. I. Yeh, J. Luba and D. Parsonage, *Adv. Protein Chem.*, 2001, **58**, 215–276.
18 N. M. Okeley and W. A. Van der Donk, *Chem. Biol.*, 2000, **7**, R159–R171.
19 C. T. Walsh, *Posttranslational Modification of Proteins: Expanding Nature's Inventory*, Roberts & Co, 2006, pp. 1–490.
20 C. T. Walsh, S. Garneau-Tsodikova and G. J. Gatto Jr, *Angew. Chem., Int. Ed.*, 2005, **44**, 7342–7372.

 

21 V. L. Davidson, *Biochemistry*, 2018, **57**, 3115–3125.
22 J. P. Klinman and F. Bonnot, *Chem. Rev.*, 2014, **114**, 4343–4365.
23 N. Fujieda, *Biosci., Biotechnol., Biochem.*, 2020, **84**, 445–454.
24 J. P. Klinman, *Acc. Chem. Res.*, 2015, **48**, 449–456.
25 U. Ermler, W. Grabarse, S. Shima, M. Goubeaud and R. K. Thauer, *Science*, 1997, **278**, 1457–1462.
26 D. Deobald, L. Adrian, C. Schöne, M. Rother and G. Layer, *Sci. Rep.*, 2018, **8**, 7404(1-12).
27 T. Wagner, J. Kahnt, U. Ermler and S. Shima, *Angew. Chem., Int. Ed.*, 2016, **55**, 10630–10633.
28 U. C. Kabisch, A. Grantzdorffer, A. Schierhorn, K. P. Rucknagel, J. R. Andreesen and A. Pich, *J. Biol. Chem.*, 1999, **274**, 8445–8454.
29 M. Wagner, D. Sonntag, R. Grimm, A. Pich, C. Eckerskorn, B. Sohling and J. R. Andreesen, *Eur. J. Biochem.*, 1999, **260**, 38–49.
30 B. Schmidt, T. Selmer, A. Ingendoh and K. von Figura, *Cell*, 1995, **82**, 271–278.
31 M. P. Cosma, S. Pepe, I. Annunziata, R. F. Newbold, M. Grompe, G. Parenti and A. Ballabio, *Cell*, 2003, **113**, 445–456.
32 T. Dierks, B. Schmidt, L. V. Borissenko, J. Peng, A. Preusser, M. Mariappan and K. von Figura, *Cell*, 2003, **113**, 435–444.
33 J. I. Yeh, A. Claiborne and W. G. J. Hol, *Biochemistry*, 1996, **35**, 9951–9957.
34 S. Nagashima, M. Nakasako, N. Dohmae, M. Tsujimura, K. Takio, M. Odaka, M. Yohda, N. Kamiya and I. Endo, *Nat. Struct. Biol.*, 1998, **5**, 347–351.
35 T. Murakami, M. Nojiri, H. Nakayama, N. Dohmae, K. Takio, M. Odaka, I. Endo, T. Nagamune and M. Yohda, *Protein Sci.*, 2000, **9**, 1024–1030.
36 I. Shin, I. Davis, K. Nieves-Merced, Y. Wang, S. McHardy and A. Liu, *Chem. Sci.*, 2021, **12**, 3984–3998.
37 D. D. Nayak, N. Mahanta, D. A. Mitchell and W. W. Metcalf, *eLife*, 2017, **6**, e29218.
38 D. D. Nayak, A. Liu, N. Agrawal, R. Rodriguez-Carerro, S.-H. Dong, D. A. Mitchell, S. K. Nair and W. W. Metcalf, *PLoS Biol.*, 2020, **18**, e3000507(1-23).
39 J. Gagsteiger, S. Jahn, L. Heidinger, L. Gericke, J. N. Andexer, T. Friedrich, C. Loenarz and G. Layer, *Angew. Chem., Int. Ed.*, 2022, **61**, e202204198.
40 J. Stubbe and W. A. van der Donk, *Chem. Rev.*, 1998, **98**, 705–762.
41 A. F. Wagner, M. Frey, F. A. Neugebauer, W. Schäfer and J. Knappe, *Proc. Natl. Acad. Sci. U. S. A.*, 1992, **89**, 996–1000.
42 A. Gendron and K. D. Allen, *Front. Microbiol.*, 2022, **13**, 867342(1-18).
43 H. Chen, Q. Gan and C. Fan, *Front. Microbiol.*, 2020, **11**, 578356(1-7).
44 B. C. Vu, A. D. Jones and J. T. Lecomte, *J. Am. Chem. Soc.*, 2002, **124**, 8544–8545.
45 X. Hou, H. Xu, Z. Deng, Y. Yan, Z. Yuan, X. Liu, Z. Su, S. Yang, Y. Zhang and Y. Rao, *Angew. Chem., Int. Ed.*, 2022, **61**, e202208772.
46 T. C. Taylor and I. Andersson, *J. Mol. Biol.*, 1997, **265**, 432–444.
47 E. Jabri, M. B. Carr, R. P. Hausinger and P. A. Karplus, *Science*, 1995, **268**, 998–1004.
48 M. M. Benning, J. M. Kuo, F. M. Raushel and H. M. Holden, *Biochemistry*, 1995, **34**, 7973–7978.
49 C. Qin, L. G. Graf, K. Striska, M. Janetzky, N. Geist, R. Specht, S. Schulze, G. J. Palm, B. Girbardt, B. Dörre, L. Berndt, S. Kemnitz, M. Doerr, U. T. Bornscheuer, M. Delcea and M. Lammers, *Nat. Commun.*, 2024, **15**, 6002.
50 B. Schwer, J. Bunkenborg, R. O. Verdin, J. S. Andersen and E. Verdin, *Proc. Natl. Acad. Sci. U. S. A.*, 2006, **103**, 10224–10229.
51 B. Desguin, T. Zhang, P. Soumillion, P. Hols, J. Hu and R. P. Hausinger, *Science*, 2015, **349**, 66–69.
52 B. Desguin, P. Soumillion, P. Hols and R. P. Hausinger, *Proc. Natl. Acad. Sci. U. S. A.*, 2016, **113**, 5598–5603.
53 W. D. Riley and E. E. Snell, *Biochemistry*, 1968, **7**, 3520–3528.
54 P. A. Recsei and E. E. Snell, *Biochemistry*, 1970, **9**, 1492–1497.
55 C. Miech, T. Dierks, T. Selmer, K. Von Figura and B. Schmidt, *J. Biol. Chem.*, 1998, **273**, 4835–4837.
56 C. Szameit, C. Miech, M. Balleininger, B. Schmidt, K. von Figura and T. Dierks, *J. Biol. Chem.*, 1999, **274**, 15375–15381.
57 A. C. Manesis, R. J. Jodts, B. M. Hoffman and A. C. Rosenzweig, *Proc. Natl. Acad. Sci. U. S. A.*, 2021, **118**, e2100680118.
58 R. Helland, A. Fjellbirkeland, O. A. Karlsen, T. Ve, J. R. Lillehaug and H. B. Jensen, *J. Biol. Chem.*, 2008, **283**, 13897–13904.
59 K. A. Johnson, T. Ve, Ø. Larsen, R. B. Pedersen, J. R. Lillehaug, H. B. Jensen, R. Helland and O. A. Karlsen, *PLoS One*, 2014, **9**, e87750.
60 S. M. Janes, D. Mu, D. Wemmer, A. J. Smith, S. Kaur, D. Maltby, A. L. Burlingame and J. P. Klinman, *Science*, 1990, **248**, 981–987.
61 B. A. Barry and G. T. Babcock, *Proc. Natl. Acad. Sci. U. S. A.*, 1987, **84**, 7099–7103.
62 A.-l Tsai, R. J. Kulmacz and G. Palmer, *J. Biol. Chem.*, 1995, **270**, 10503–10508.
63 Z. Deng, H. Su, X. Hou, H. Xu, Z. Yuan, X. Sheng and Y. Rao, *ACS Catal.*, 2024, **14**, 797–811.
64 M. Lammers, *Front. Microbiol.*, 2021, **12**, 757179.
65 A. T. Blasl, S. Schulze, C. Qin, L. G. Graf, R. Vogt and M. Lammers, *Biol. Chem.*, 2022, **403**, 151–194.
66 J. G. Gardner, F. J. Grundy, T. M. Henkin and J. C. Escalante-Semerena, *J. Bacteriol.*, 2006, **188**, 5460–5468.
67 J. Nevarez, A. Turmo, J. Hu and R. P. Hausinger, *ChemCatChem*, 2020, **12**, 4242–4254.
68 S. Gatreddi, S. Chatterjee, A. Turmo, J. Hu and R. P. Hausinger, *Crit. Rev. Biochem. Mol. Biol.*, 2025, 1–16.
69 J. A. Rankin, S. Chatterjee, Z. Tariq, S. Lagishetty, B. Desguin, J. Hu and R. P. Hausinger, *Proc. Natl. Acad. Sci. U. S. A.*, 2021, **118**, e2106202118.
70 S. Chatterjee, J. L. Nevarez, J. A. Rankin, J. Hu and R. P. Hausinger, *Biochemistry*, 2023, **62**, 3096–3104.

71 M. Fellner, B. Desguin, R. P. Hausinger and J. Hu, *Proc. Natl. Acad. Sci. U. S. A.*, 2017, **114**, 9074–9079.
72 M. Fellner, J. A. Rankin, B. Desguin, J. Hu and R. P. Hausinger, *Biochemistry*, 2018, **57**, 5513–5523.
73 M. Fellner, K. G. Huizenga, R. P. Hausinger and J. Hu, *Sci. Rep.*, 2020, **10**, 5830(1-9).
74 S. Chatterjee, K. F. Parson, B. T. Ruotolo, J. McCracken, J. Hu and R. P. Hausinger, *J. Biol. Chem.*, 2022, **298**, 102131(1-14).
75 A. Turmo, J. Hu and R. P. Hausinger, *Metallomics*, 2022, **14**, mfac014(1–8).
76 B. Desguin, P. Goffin, E. Viaene, M. Kleerebezem, V. Martin-Diaconescu, M. J. Maroney, J.-P. Declercq, P. Soumillion and P. Hols, *Nat. Commun.*, 2014, **5**, 3615(1-12).
77 R. E. Treviño and H. S. Shafaat, *Curr. Opin. Chem. Biol.*, 2022, **67**, 102110(1-8).
78 V. Sanchez-Torres and T. K. Wood, *Microb. Biotechnol.*, 2024, **17**, e70000(1-7).
79 Y. Miyazaki, K. Oohora and T. Hayashi, *Chem. Soc. Rev.*, 2022, **51**, 1629–1639.
80 S. Shima, M. Krueger, T. Weinert, U. Demmer, J. Kahnt, R. K. Thauer and U. Ermler, *Nature*, 2012, **481**, 98–101.
81 T. Wagner, C.-E. Wegner, J. Kahnt, U. Ermler and S. Shima, *J. Bacteriol.*, 2017, **199**, e00197-17(1-15).
82 C. J. Hahn, O. N. Lemaire, J. Kahnt, S. Engilberge, G. Wegener and T. Wagner, *Science*, 2021, **373**, 118–121.
83 T. Selmer, J. Kahnt, M. Goubeaud, S. Shima, W. Grabarse, U. Ermler and R. K. Thauer, *J. Biol. Chem.*, 2000, **275**, 3755–3760.
84 W. Grabarse, F. Mahlert, S. Shima, R. K. Thauer and U. Ermler, *J. Mol. Biol.*, 2000, **303**, 329–344.
85 C. D. Fyfe, N. Bernardo-García, L. Fradale, S. Grimaldi, A. Guillot, C. Brewee, L. M. G. Chavas, P. Legrand, A. Benjdia and O. Berteau, *Nature*, 2022, **602**, 336–342.
86 M. I. Radle, D. V. Miller, T. N. Laremore and S. J. Booker, *J. Biol. Chem.*, 2019, **294**, 11712–11725.
87 H. J. Sofia, G. Chen, B. G. Hetzler, J. F. Reyes-Spindola and N. E. Miller, *Nucleic Acids Res.*, 2001, **29**, 1097–1106.
88 S. J. Booker and T. L. Grove, *F1000 Biol. Rep.*, 2010, **2**, 52.
89 J. M. Kuchenreuther, W. K. Myers, T. A. Stich, S. J. George, Y. Nejatyjahromy, J. R. Swartz and R. D. Britt, *Science*, 2013, **342**, 472–475.
90 J. Wang, R. P. Woldring, G. D. Román-Meléndez, A. M. McClain, B. R. Alzua and E. N. Marsh, *ACS Chem. Biol.*, 2014, **9**, 1929–1938.
91 Z. Lyu, N. Shao, C.-W. Chou, H. Shi, R. Patel, E. C. Duin and W. B. William, *J. Bacteriol.*, 2020, **202**, e00654-19(1-18).
92 G. E. Kenney and A. C. Rosenzweig, *J. Biol. Chem.*, 2018, **293**, 4606–4615.
93 L. M. R. Jensen, R. Sanishvili, V. L. Davidson and C. M. Wilmot, *Science*, 2010, **327**, 1392–1394.
94 X. Li, R. Fu, A. Liu and V. L. Davidson, *Biochemistry*, 2008, **47**, 2908–2912.
95 M. Feng, L. M. R. Jensen, E. T. Yukl, X. Wei, A. Liu, C. M. Wilmot and V. L. Davidson, *Biochemistry*, 2012, **51**, 1598–1606.
96 E. T. Yukl, F. Liu, J. Krzystek, S. Shin, L. M. R. Jensen, V. L. Davidson, C. M. Wilmot and A. Liu, *Proc. Natl. Acad. Sci. U. S. A.*, 2013, **110**, 4569–4573.
97 V. L. Davidson and A. Liu, *Biochim. Biophys. Acta*, 2012, **1824**, 1299–1305.
98 X. Li, R. Fu, S. Lee, C. Krebs, V. L. Davidson and A. Liu, *Proc. Natl. Acad. Sci. U. S. A.*, 2008, **105**, 8597–8600.
99 J. Geng, K. Dornevil, V. L. Davidson and A. Liu, *Proc. Natl. Acad. Sci. U. S. A.*, 2013, **110**, 9639–9644.
100 J. Geng, I. Davis and A. Liu, *Angew. Chem., Int. Ed.*, 2015, **54**, 3692–3696.
101 N. A. Tarboush, L. M. R. Jensen, E. T. Yukl, J. Geng, A. Liu, C. M. Wilmot and V. L. Davidson, *Proc. Natl. Acad. Sci. U. S. A.*, 2011, **108**, 16956–16961.
102 J. Geng, I. Davis, F. Liu and A. Liu, *J. Biol. Inorg. Chem.*, 2014, **19**, 1057–1067.
103 A. C. Manesis, J. W. Slater, K. Cantave, J. Martin Bollinger, Jr., C. Krebs and A. C. Rosenzweig, *Biochemistry*, 2023, **62**, 1082–1092.
104 K. Rizzolo, S. E. Cohen, A. C. Weitz, M. M. López Muñoz, M. P. Hendrich, C. L. Drennan and S. J. Elliott, *Nat. Commun.*, 2019, **10**(1101), 1–10.
105 T. W. Stone and L. G. Darlington, *Nat. Rev. Drug Discovery*, 2002, **1**, 609–620.
106 R. Schwarcz, J. P. Bruno, P. J. Muchowski and H. Q. Wu, *Nat. Rev. Neurosci.*, 2012, **13**, 465–477.
107 A. Newton, L. McCann, L. Huo and A. Liu, *Metabolites*, 2023, **13**, 500(1-13).
108 I. Davis and A. Liu, *Expert Rev. Neurother.*, 2015, **15**, 719–721.
109 E. M. Shepard and D. M. Dooley, *J. Biol. Inorg. Chem.*, 2006, **11**, 1039–1048.
110 S. X. Wang, M. Mure, K. F. Medzihradszky, A. L. Burlingame, D. E. Brown, D. M. Dooley, A. J. Smith, H. M. Kagan and J. P. Klinman, *Science*, 1996, **273**, 1078–1084.
111 M. R. Parsons, M. A. Convery, C. M. Wilmot, K. D. Yadav, V. Blakeley, A. S. Corner, S. E. Phillips, M. J. McPherson and P. F. Knowles, *Structure*, 1995, **3**, 1171–1184.
112 V. Kumar, D. M. Dooley, H. C. Freeman, J. M. Guss, I. Harvey, M. A. McGuirl, M. C. Wilce and V. M. Zubak, *Structure*, 1996, **4**, 943–955.
113 L. Luhová, L. Slavík, I. Frébort, M. Sebela, L. Zajoncová and P. Peč, *J. Enzyme Inhib.*, 1996, **10**, 251–262.
114 M. C. J. Wilce, D. M. Dooley, H. C. Freeman, J. M. Guss, H. Matsunami, W. S. McIntire, C. E. Ruggiero, K. Tanizawa and H. Yamaguchi, *Biochemistry*, 1997, **36**, 16116–16133.
115 R. Li, J. P. Klinman and F. S. Mathews, *Structure*, 1998, **6**, 293–307.
116 M. Lunelli, M. L. Di Paolo, M. Biadene, V. Calderone, R. Battistutta, M. Scarpa, A. Rigo and G. Zanotti, *J. Mol. Biol.*, 2005, **346**, 991–1004.
117 A. P. Duff, A. E. Cohen, P. J. Ellis, J. A. Kuchar, D. B. Langley, E. M. Shepard, D. M. Dooley, H. C. Freeman and J. M. Guss, *Biochemistry*, 2003, **42**, 15148–15157.

 

118 M. Kim, T. Okajima, S. Kishishita, M. Yoshimura, A. Kawamori, K. Tanizawa and H. Yamaguchi, *Nat. Struct. Biol.*, 2002, **9**, 591–596.
119 C. M. Wilmot, J. M. Murray, G. Alton, M. R. Parsons, M. A. Convery, V. Blakeley, A. S. Corner, M. M. Palcic, P. F. Knowles, M. J. McPherson and S. E. Phillips, *Biochemistry*, 1997, **36**, 1608–1620.
120 T. Murakawa, S. Baba, Y. Kawano, H. Hayashi, T. Yano, T. Kumasaka, M. Yamamoto, K. Tanizawa and T. Okajima, *Proc. Natl. Acad. Sci. U. S. A.*, 2019, **116**, 135–140.
121 A. Ehrenberg and P. Reichard, *J. Biol. Chem.*, 1972, **247**, 3485–3488.
122 B. M. Sjöberg and P. Reichard, *J. Biol. Chem.*, 1977, **252**, 536–541.
123 B. M. Sjöberg, P. Reichard, A. Gräslund and A. Ehrenberg, *J. Biol. Chem.*, 1978, **253**, 6863–6865.
124 P. Reichard and A. Ehrenberg, *Science*, 1983, **221**, 514–519.
125 J. Stubbe and D. G. Nocera, *J. Am. Chem. Soc.*, 2021, **143**, 13463–13472.
126 S. J. Booker, *Biochim. Biophys. Acta*, 2012, **1824**, 1151–1153.
127 J. M. Bollinger, Jr., D. E. Edmondson, B. H. Huynh, J. Filley, J. R. Norton and J. Stubbe, *Science*, 1991, **253**, 292–298.
128 N. Ravi, J. M. Bollinger, Jr., B. H. Huynh, J. Stubbe and D. E. Edmondson, *J. Am. Chem. Soc.*, 1994, **116**, 8007–8014.
129 N. Mitić, M. D. Clay, L. Saleh, J. M. Bollinger and E. I. Solomon, *J. Am. Chem. Soc.*, 2007, **129**, 9049–9065.
130 A. Liu, S. Pötsch, A. Davydov, A. L. Barra, H. Rubin and A. Gräslund, *Biochemistry*, 1998, **37**, 16369–16377.
131 A. Liu, A.-L. Barra, H. Rubin, G. Lu and A. Gräslund, *J. Am. Chem. Soc.*, 2000, **122**, 1974–1978.
132 G. Kang, A. T. Taguchi, J. Stubbe and C. L. Drennan, *Science*, 2020, **368**, 424–427.
133 B. M. Sjöberg, A. Gräslund and F. Eckstein, *J. Biol. Chem.*, 1983, **258**, 8060–8067.
134 M. Ator, S. P. Salowe, J. Stubbe, M. H. Emptage and M. J. Robins, *J. Am. Chem. Soc.*, 1984, **106**, 1886–1887.
135 B. L. Greene, G. Kang, C. Cui, M. Bennati, D. G. Nocera, C. L. Drennan and J. Stubbe, *Annu. Rev. Biochem.*, 2020, **89**, 45–75.
136 R. P. Pesavento and W. A. Van Der Donk, *Advances in Protein Chemistry*, Academic Press, 2001, vol. 58, pp. 317–385.
137 R. J. Debus, B. A. Barry, I. Sithole, G. T. Babcock and L. McIntosh, *Biochemistry*, 1988, **27**, 9071–9074.
138 S. Gerken, K. Brettel, E. Schlodder and H. T. Witt, *FEBS Lett.*, 1988, **237**, 69–75.
139 K. Saito, A. W. Rutherford and H. Ishikita, *Proc. Natl. Acad. Sci. U. S. A.*, 2013, **110**, 7690–7695.
140 R. Dietz, W. Nastainczyk and H. H. Ruf, *Eur. J. Biochem.*, 1988, **171**, 321–328.
141 A. L. Tsai, G. Palmer and R. J. Kulmacz, *J. Biol. Chem.*, 1992, **267**, 17753–17759.
142 A.-L. Tsai and R. J. Kulmacz, *Prostaglandins Other Lipid Mediators*, 2000, **62**, 231–254.
143 V. Unkrig, F. A. Neugebauer and J. Knappe, *Eur. J. Biochem.*, 1989, **184**, 723–728.
144 E. Mulliez, M. Fontecave, J. Gaillard and P. Reichard, *J. Biol. Chem.*, 1993, **268**, 2296–2299.
145 A. Becker, K. Fritz-Wolf, W. Kabsch, J. Knappe, S. Schultz and A. F. Volker Wagner, *Nat. Chem. Biol.*, 1999, **6**, 969–975.
146 D. T. Logan, J. Andersson, B. M. Sjöberg and P. Nordlund, *Science*, 1999, **283**, 1499–1504.
147 E. Torrents, G. Buist, A. Liu, R. Eliasson, J. Kok, I. Gibert, A. Gräslund and P. Reichard, *J. Biol. Chem.*, 2000, **275**, 2463–2471.
148 J. Knappe and A. F. Wagner, *Adv. Protein Chem.*, 2001, **58**, 277–315.
149 A. Liu and A. Gräslund, *J. Biol. Chem.*, 2000, **275**, 12367–12373.
150 D. T. Logan, E. Mulliez, K. M. Larsson, S. Bodevin, M. Atta, P. E. Garnaud, B. M. Sjoberg and M. Fontecave, *Proc. Natl. Acad. Sci. U. S. A.*, 2003, **100**, 3826–3831.
151 M. Frey, M. Rothe, A. F. Wagner and J. Knappe, *J. Biol. Chem.*, 1994, **269**, 12432–12437.
152 J. L. Vey, J. Yang, M. Li, W. E. Broderick, J. B. Broderick and C. L. Drennan, *Proc. Natl. Acad. Sci. U. S. A.*, 2008, **105**, 16137–16141.
153 E. M. Shepard and J. B. Broderick, in *Comprehensive Natural Products II*, ed. H.-W. Liu and L. Mander, Elsevier, Oxford, 2010, pp. 625–661.
154 D. S. King and P. Reichard, *Biochem. Biophys. Res. Commun.*, 1995, **206**, 731–735.
155 A. Becker and W. Kabsch, *J. Biol. Chem.*, 2002, **277**, 40036–40042.
156 J. Stubbe, *Proc. Natl. Acad. Sci. U. S. A.*, 1998, **95**, 2723–2724.
157 J. Stubbe and P. Riggs-Gelasco, *Trends Biochem. Sci.*, 1998, **23**, 438–443.
158 C. L. Atkin, L. Thelander, P. Reichard and G. Lang, *J. Biol. Chem.*, 1973, **248**, 7464–7472.
159 U. Griepenburg, G. Lassmann and G. Auling, *Free Radical Res.*, 1996, **24**, 473–481.
160 S. Licht, G. J. Gerfen and J. Stubbe, *Science*, 1996, **271**, 477–481.
161 Y. Tamao and R. L. Blakley, *Biochemistry*, 1973, **12**, 24–34.
162 W. H. Orme-Johnson, H. Beinert and R. L. Blakley, *J. Biol. Chem.*, 1974, **249**, 2338–2343.
163 P. Reichard, *Science*, 1993, **260**, 1773–1777.
164 J. C. Cáceres, C. A. Bailey, K. Yokoyama and B. L. Greene, *Methods Enzymol.*, 2022, **662**, 119–141.
165 T. Nauser, S. Dockheer, R. Kissner and W. H. Koppenol, *Biochemistry*, 2006, **45**, 6038–6043.
166 T. Yonetani and H. Schleyer, *J. Biol. Chem.*, 1966, **241**, 3240–3243.
167 M. Sivaraja, D. B. Goodin, M. Smith and B. M. Hoffman, *Science*, 1989, **245**, 738–740.
168 T. M. Payne, E. F. Yee, B. Dzikovski and B. R. Crane, *Biochemistry*, 2016, **55**, 4807–4822.
169 H. Mei, K. Wang, N. Peffer, G. Weatherly, D. S. Cohen, M. Miller, G. Pielak, B. Durham and F. Millett, *Biochemistry*, 1999, **38**, 6846–6854.

170 K. Wang, H. Mei, L. Geren, M. A. Miller, A. Saunders, X. Wang, J. L. Waldner, G. J. Pielak, B. Durham and F. Millett, *Biochemistry*, 1996, **35**, 15107–15119.
171 C. A. Bonagura, M. Sundaramoorthy, H. S. Pappa, W. R. Patterson and T. L. Poulos, *Biochemistry*, 1996, **35**, 6107–6115.
172 W. R. Patterson and T. L. Poulos, *Biochemistry*, 1995, **34**, 4331–4341.
173 W. R. Patterson, T. L. Poulos and D. B. Goodin, *Biochemistry*, 1995, **34**, 4342–4345.
174 V. S. Jasion, J. A. Polanco, Y. T. Meharenna, H. Li and T. L. Poulos, *J. Biol. Chem.*, 2011, **286**, 24608–24615.
175 T. L. Poulos, J. S. Kim and V. C. Murarka, *J. Biol. Inorg. Chem.*, 2022, **27**, 229–237.
176 K. Lerch, *J. Biol. Chem.*, 1982, **257**, 6414–6419.
177 N. Fujieda, T. Ikeda, M. Murata, S. Yanagisawa, S. Aono, K. Ohkubo, S. Nagao, T. Ogura, S. Hirota, S. Fukuzumi, Y. Nakamura, Y. Hata and S. Itoh, *J. Am. Chem. Soc.*, 2011, **133**, 1180–1183.
178 N. Fujieda, K. Umakoshi, Y. Ochi, Y. Nishikawa, S. Yanagisawa, M. Kubo, G. Kurisu and S. Itoh, *Angew. Chem.*, 2020, **132**, 13487–13492.
179 C. Gielens, N. De Geest, X.-Q. Xin, B. Devreese, J. Van Beeumen and G. Preaux, *Eur. J. Biochem.*, 1997, **248**, 879–888.
180 M. E. Cuff, K. I. Miller, K. E. Van Holde and W. A. Hendrickson, *J. Mol. Biol.*, 1998, **278**, 855–870.
181 T. Klabunde, C. Eicken, J. C. Sacchettini and B. Krebs, *Nat. Struct. Biol.*, 1998, **5**, 1084–1090.
182 M. Wensien, F. R. von Pappenheim, L.-M. Funk, P. Kloskowski, U. Curth, U. Diederichsen, J. Uranga, J. Ye, P. Fang, K.-T. Pan, H. Urlaub, R. A. Mata, V. Sautner and K. Tittmann, *Nature*, 2021, **593**, 460–464.
183 A. Satoh, J.-K. Kim, I. Miyahara, B. Devreese, I. Vandenberghe, A. Hacisalihoglu, T. Okajima, S. I. Kuroda, O. Adachi, J. A. Duine, J. Van Beeumen, K. Tanizawa and K. Hirotsu, *J. Biol. Chem.*, 2002, **277**, 2830–2834.
184 S. Okazaki, S. Nakano, D. Matsui, S. Akaji, K. Inagaki and Y. Asano, *J. Biochem.*, 2013, **154**, 233–236.
185 A. Andreo-Vidal, K. J. Mamounis, E. Sehanobish, D. Avalos, J. C. Campillo-Brocal, A. Sanchez-Amat, E. T. Yukl and V. L. Davidson, *Biochemistry*, 2018, **57**, 1155–1165.
186 M. M. Whittaker and J. W. Whittaker, *J. Biol. Chem.*, 1990, **265**, 9610–9613.
187 N. Ito, S. E. V. Phillips, C. Stevens, Z. B. Ogel, M. J. McPherson, J. N. Keen, K. D. S. Yadav and P. F. Knowles, *Nature*, 1991, **350**, 87–90.
188 J. G. McCoy, L. J. Bailey, E. Bitto, C. A. Bingman, D. J. Aceti, B. G. Fox and G. N. Phillips, *Proc. Natl. Acad. Sci. U. S. A.*, 2006, **103**, 3084–3089.
189 A. K. Chaplin, M. L. Petrus, G. Mangiameli, M. A. Hough, D. A. Svistunenko, P. Nicholls, D. Claessen, E. Vijgenboom and J. A. Worrall, *Biochem. J.*, 2015, **469**, 433–444.
190 R. Schnell, T. Sandalova, U. Hellman, Y. Lindqvist and G. Schneider, *J. Biol. Chem.*, 2005, **280**, 27319–27328.
191 K. M. Polyakov, K. M. Boyko, T. V. Tikhonova, A. Slutsky, A. N. Antipov, R. A. Zvyagilskaya, A. N. Popov, G. P. Bourenkov, V. S. Lamzin and V. O. Popov, *J. Mol. Biol.*, 2009, **389**, 846–862.
192 C. Ostermeier, A. Harrenga, U. Ermler and H. Michel, *Proc. Natl. Acad. Sci. U. S. A.*, 1997, **94**, 10547–10553.
193 M. A. Ehudin, L. Senft, A. Franke, I. Ivanović-Burmazović and K. D. Karlin, *J. Am. Chem. Soc.*, 2019, **141**, 10632–10643.
194 S. Yoshikawa, K. Shinzawa-itoh, R. Nakashima, R. Yaono, E. Yamashita, N. Inoue, M. Yao, M. J. Fei, C. P. Libeu, T. Mizushima, H. Yamaguchi, T. Tomizaki and T. Tsukihara, *Science*, 1998, **280**, 1723–1729.
195 A. Buzy, V. Bracchi, R. Sterjiades, J. Chroboczek, P. Thibault, J. Gagnon, H. M. Jouve and G. Hudry-Clergeon, *J. Protein Chem.*, 1995, **14**, 59–72.
196 J. Bravo, I. Fita, J. C. Ferrer, W. Ens, A. Hillar, J. Switala and P. C. Loewen, *Protein Sci.*, 1997, **6**, 1016–1023.
197 W. S. McIntire, D. E. Wemmer, A. Chistoserdov and M. E. Lidstrom, *Science*, 1991, **252**, 817–824.
198 L. Chen, F. S. Mathews, V. L. Davidson, E. G. Huizinga, F. M. D. Vellieux, J. A. Duine and W. G. J. Hol, *FEBS Lett.*, 1991, **287**, 163–166.
199 L. Chen, R. C. Durley, F. S. Mathews and V. L. Davidson, *Science*, 1994, **264**, 86–90.
200 S. Datta, Y. Mori, K. Takagi, K. Kawaguchi, Z.-W. Chen, T. Okajima, S. I. Kuroda, T. Ikeda, K. Kano, K. Tanizawa and F. S. Mathews, *Proc. Natl. Acad. Sci. U. S. A.*, 2001, **98**, 14268–14273.
201 J. G. Hauge, *J. Biol. Chem.*, 1964, **239**, 3630–3639.
202 M. D. Chacón-Verdú, J. C. Campillo-Brocal, P. Lucas-Elío, V. L. Davidson and A. Sánchez-Amat, *Biochim. Biophys. Acta*, 2015, **1854**, 1123–1131.
203 O. T. Magnusson, H. Toyama, M. Saeki, A. Rojas, J. C. Reed, R. C. Liddington, J. P. Klinman and R. Schwarzenbacher, *Proc. Natl. Acad. Sci. U. S. A.*, 2004, **101**, 7913–7918.
204 T. Kasahara and T. Kato, *Nature*, 2003, **422**, 832.
205 S. A. Salisbury, H. S. Forrest, W. B. Cruse and O. Kennard, *Nature*, 1979, **280**, 843–844.
206 Y. Wang, M. E. Graichen, A. Liu, A. R. Pearson, C. M. Wilmot and V. L. Davidson, *Biochemistry*, 2003, **42**, 7318–7325.
207 R. Fu, F. Liu, V. L. Davidson and A. Liu, *Biochemistry*, 2009, **48**, 11603–11605.
208 E. T. Yukl and V. L. Davidson, *Arch. Biochem. Biophys.*, 2018, **654**, 40–46.
209 T. Oozeki, T. Nakai, K. Kozakai, K. Okamoto, S. I. Kuroda, K. Kobayashi, K. Tanizawa and T. Okajima, *Nat. Commun.*, 2021, **12**, 933.
210 M. D. Chacón-Verdú, D. Gómez, F. Solano, P. Lucas-Elío and A. Sánchez-Amat, *Appl. Microbiol. Biotechnol.*, 2014, **98**, 2981–2989.
211 X. Zhang, Q. Wang, J. Wu, J. Wang, Y. Shi and M. Liu, *Proc. Natl. Acad. Sci. U. S. A.*, 2018, **115**, 3828–3833.
212 A. A. Meier, K. Kuczera and M. Mure, *Int. J. Mol. Sci.*, 2022, **23**, 13385(1-13).

 

213 F. Rabe von Pappenheim, M. Wensien, J. Ye, J. Uranga, I. Irisarri, J. de Vries, L.-M. Funk, R. A. Mata and K. Tittmann, *Nat. Chem. Biol.*, 2022, **18**, 368–375.
214 J. Ye, S. Bazzi, T. Fritz, K. Tittmann, R. A. Mata and J. Uranga, *Angew. Chem., Int. Ed.*, 2023, **62**, e202304163.
215 Y. Wang and A. Liu, *Chem. Soc. Rev.*, 2020, **49**, 4906–4925.
216 N. Masson, T. P. Keeley, B. Giuntoli, M. D. White, M. L. Puerta, P. Perata, R. J. Hopkinson, E. Flashman, F. Licausi and P. J. Ratcliffe, *Science*, 2019, **365**, 65–69.
217 Y. Wang, I. Shin, J. Li and A. Liu, *J. Biol. Chem.*, 2021, **297**, 101176(1-10).
218 R. L. Fernandez, L. D. Elmendorf, R. W. Smith, C. A. Bingman, B. G. Fox and T. C. Brunold, *Biochemistry*, 2021, **60**, 3728–3737.
219 Y. Wang, I. Davis, Y. Chan, S. G. Naik, W. P. Griffith and A. Liu, *J. Biol. Chem.*, 2020, **295**, 11789–11802.
220 J. E. Dominy, Jr., C. R. Simmons, L. L. Hirschberger, J. Hwang, R. M. Coloso and M. H. Stipanuk, *J. Biol. Chem.*, 2007, **282**, 25189–25198.
221 M. H. Stipanuk, *J. Nutr.*, 2020, **150**, 2494s–2505s.
222 D. M. Gunawardana, K. C. Heathcote and E. Flashman, *FEBS J.*, 2022, **289**, 5426–5439.
223 C. R. Simmons, Q. Liu, Q. Huang, Q. Hao, T. P. Begley, P. A. Karplus and M. H. Stipanuk, *J. Biol. Chem.*, 2006, **281**, 18723–18733.
224 C. W. Njeri and H. R. Ellis, *Arch. Biochem. Biophys.*, 2014, **558**, 61–69.
225 J. Li, T. Koto, I. Davis and A. Liu, *Biochemistry*, 2019, **58**, 2218–2227.
226 J. E. Dominy, J. Hwang, S. Guo, L. L. Hirschberger, S. Zhang and M. H. Stipanuk, *J. Biol. Chem.*, 2008, **283**, 12188–12201.
227 J. Li, R. Duan and A. Liu, *J. Am. Chem. Soc.*, 2024, **146**, 18292–18297.
228 D. T. Yin, S. Urresti, M. Lafond, E. M. Johnston, F. Derikvand, L. Ciano, J. G. Berrin, B. Henrissat, P. H. Walton, G. J. Davies and H. Brumer, *Nat. Commun.*, 2015, **6**, 10197.
229 J. W. Whittaker, *Chem. Rev.*, 2003, **103**, 2347–2363.
230 K. Clark, J. E. Penner-Hahn, M. M. Whittaker and J. W. Whittaker, *J. Am. Chem. Soc.*, 1990, **112**, 6433–6434.
231 M. S. Rogers and D. M. Dooley, *Adv. Protein Chem.*, 2001, **58**, 387–436.
232 P. F. Knowles and N. Ito, *Perspect. Bioinorg. Chem.*, 1993, **2**, 207–244.
233 M. J. McPherson, C. Stevens, A. J. Baron, Z. B. Ogel, K. Seneviratne, C. Wilmot, N. Ito, I. Brocklebank, S. E. V. Phillips and P. F. Knowles, *Biochem. Soc. Trans.*, 1993, **21**, 752–756.
234 Y. Wang, J. L. DuBois, B. Hedman, K. O. Hodgson and T. D. Stack, *Science*, 1998, **279**, 537–540.
235 J. W. Whittaker and M. M. Whittaker, *Pure & Appl. Chem.*, 1998, **70**, 903–910.
236 A. J. Baron, C. Stevens, C. Wilmot, P. F. Knowles, S. E. V. Phillips and M. J. McPherson, *Biochem. Soc. Trans.*, 1993, **21**, 319S–319S.
237 M. M. Whittaker, P. J. Kersten, D. Cullen and J. W. Whittaker, *J. Biol. Chem.*, 1999, **274**, 36226–36232.
238 Q. Zhou, M. Hu, W. Zhang, L. Jiang, S. Perrett, J. Zhou and J. Wang, *Angew. Chem., Int. Ed.*, 2013, **52**, 1203–1207.
239 R. E. Cowley, J. Cirera, M. F. Qayyum, D. Rokhsana, B. Hedman, K. O. Hodgson, D. M. Dooley and E. I. Solomon, *J. Am. Chem. Soc.*, 2016, **138**, 13219–13229.
240 K. S. Yang, L. R. Blankenship, S.-T. A. Kuo, Y. J. Sheng, P. Li, C. A. Fierke, D. H. Russell, X. Yan, S. Xu and W. R. Liu, *ACS Chem. Biol.*, 2023, **18**, 449–455.
241 T. F. Schwede, J. Retey and G. E. Schulz, *Biochemistry*, 1999, **38**, 5355–5361.
242 B. Schuster and J. Retey, *FEBS Lett.*, 1994, **349**, 252–254.
243 K. T. Watts, B. N. Mijts, P. C. Lee, A. J. Manning and C. Schmidt-Dannert, *Chem. Biol.*, 2006, **13**, 1317–1326.
244 T. Bertrand, N. A. J. Eady, J. N. Jones, Jesmin, J. M. Nagy, B. Jamart-Gregoire, E. L. Raven and K. A. Brown, *J. Biol. Chem.*, 2004, **279**, 38991–38999.
245 M. Ormö, A. B. Cubitt, K. Kallio, L. A. Gross, R. Y. Tsien and S. J. Remington, *Science*, 1996, **273**, 1392–1395.
246 B. Langer, M. Langer and J. Rétey, *Adv. Protein Chem.*, 2001, **58**, 175–214.
247 T. Scior, I. Meneses Morales, S. J. Garcés Eisele, D. Domeyer and S. Laufer, *Arch. Pharm.*, 2002, **335**, 511–525.
248 A. Liu, *Crit. Rev. Biochem. Mol. Biol.*, 2024, **59**, 434–446.
249 Y. Yamada, T. Fujiwara, T. Sato, N. Igarashi and N. Tanaka, *Nat. Struct. Biol.*, 2002, **9**, 691–695.
250 R. A. Ghiladi, G. M. Knudsen, K. F. Medzihradszky and P. R. O. de Montellano, *J. Biol. Chem.*, 2005, **280**, 22651–22663.
251 R. A. Ghiladi, K. F. Medzihradszky and P. R. Ortiz de Montellano, *Biochemistry*, 2005, **44**, 15093–15105.
252 O. J. Njuma, I. Davis, E. N. Ndontsa, J. R. Krewall, A. Liu and D. C. Goodwin, *J. Biol. Chem.*, 2017, **292**, 18408–18421.
253 X. Zhao, J. Suarez, A. Khajo, S. Yu, L. Metlitsky and R. S. Magliozzo, *J. Am. Chem. Soc.*, 2010, **132**, 8268–8269.
254 J. Li, R. Duan, E. S. Traore, R. C. Nguyen, I. Davis, W. P. Griffth, D. C. Goodwin, A. A. Jarzecki and A. Liu, *Angew. Chem., Int. Ed.*, 2024, **63**, e202407018(1-10).
255 P. C. Loewen, X. Carpena, P. Vidossich, I. Fita and C. Rovira, *J. Am. Chem. Soc.*, 2014, **136**, 7249–7252.
256 X. Carpena, S. Loprasert, S. Mongkolsuk, J. Switala, P. C. Loewen and I. Fita, *J. Mol. Biol.*, 2003, **327**, 475–489.
257 W. Zhu and J. P. Klinman, *Curr. Opin. Chem. Biol.*, 2020, **59**, 93–103.
258 I. Shin, Y. Wang and A. Liu, *Proc. Natl. Acad. Sci. U. S. A.*, 2021, **118**, e210656(1-10).
259 B. B. Wenke, J. T. Lecomte, A. Héroux and J. L. Schlessman, *Proteins*, 2014, **82**, 528–534.
260 H. J. Nothnagel, M. R. Preimesberger, M. P. Pond, B. Y. Winer, E. M. Adney and J. T. Lecomte, *J. Biol. Inorg. Chem.*, 2011, **16**, 539–552.
261 H. M. Cheng, H. Yuan, X. J. Wang, J. K. Xu, S. Q. Gao, G. B. Wen, X. Tan and Y. W. Lin, *J. Inorg. Biochem.*, 2018, **182**, 141–149.

262 S. L. Rice, M. R. Preimesberger, E. A. Johnson and J. T. J. Lecomte, *J. Inorg. Biochem.*, 2014, **141**, 198–207.
263 S. Uppal, S. Salhotra, N. Mukhi, F. K. Zaidi, M. Seal, S. G. Dey, R. Bhat and S. Kundu, *J. Biol. Chem.*, 2015, **290**, 1979–1993.
264 M. R. Preimesberger, E. A. Johnson, D. B. Nye and J. T. J. Lecomte, *J. Inorg. Biochem.*, 2017, **177**, 171–182.
265 T. S. Young, I. Ahmad, J. A. Yin and P. G. Schultz, *J. Mol. Biol.*, 2010, **395**, 361–374.
266 E. C. Minnihan, M. R. Seyedsayamdost and J. Stubbe, *Biochemistry*, 2009, **48**, 12125–12132.
267 M. R. Seyedsayamdost, J. Xie, C. T. Y. Chan, P. G. Schultz and J. Stubbe, *J. Am. Chem. Soc.*, 2007, **129**, 15060–15071.
268 Z. Birch-Price, F. J. Hardy, T. M. Lister, A. R. Kohn and A. P. Green, *Chem. Rev.*, 2024, **124**, 8740–8786.
269 T. Hayashi, Generation of functionalized biomolecules using hemoprotein matrices with small protein cavities for incorporation of cofactors, In *Coordination Chemistry in Protein Cages: Principles, Design, and Applications*, ed T. Ueno and Y. Watanabe, John Wiley & Sons, Inc., 1st ed., 2013.
270 T. Matsuo and T. Hayashi, *J. Porphyrins Phthalocyanines*, 2009, **13**, 1082–1089.
271 T. Hayashi, Y. Sano and A. Onoda, *Isr. J. Chem.*, 2015, **55**, 76–84.
272 K. Oohora, A. Onoda and T. Hayashi, *Acc. Chem. Res.*, 2019, **52**, 945–954.
273 M. Uchimiya and A. T. Stone, *Chemosphere*, 2009, **77**, 451–458.
274 A. E. Wendlandt and S. S. Stahl, *Angew. Chem., Int. Ed.*, 2015, **54**, 14638–14658.
275 T. S. Eckert and T. C. Bruice, *J. Am. Chem. Soc.*, 1983, **105**, 4431–4441.
276 T. Xu, M. D. Wodrich, R. Scopelliti, C. Corminboeuf and X. Hu, *Proc. Natl. Acad. Sci. U. S. A.*, 2017, **114**, 1242–1245.
277 R. Shi, M. D. Wodrich, H. J. Pan, F. F. Tirani and X. Hu, *Angew. Chem., Int. Ed.*, 2019, **58**, 16869–16872.
278 J. A. Rankin, R. C. Mauban, M. Fellner, B. Desguin, J. McCracken, J. Hu, S. A. Varganov and R. P. Hausinger, *Biochemistry*, 2018, **57**, 3244–3251.
279 S. Itoh, M. Taki and S. Fukuzumi, *Coord. Chem. Rev.*, 2000, **198**, 3–20.
280 X. H. Liu, H. Y. Yu, J. Y. Huang, J. H. Su, C. Xue, X. T. Zhou, Y. R. He, Q. He, D. J. Xu, C. Xiong and H. B. Ji, *Chem. Sci.*, 2022, **13**, 9560–9568.
281 P. Chaudhuri, M. Hess, T. Weyhermüller and K. Wieghardt, *Angew. Chem., Int. Ed.*, 1999, **38**, 1095–1098.
282 E. saint-Aman, S. p Me′nage, J. L. Pierre, E. Defrancq and G. Gellon, *New J. Chem.*, 1998, **22**, 393–394.
283 N. Kitajima, K. Whang, Y. Moro-oka, A. Uchida and Y. Sasada, *J. Chem. Soc., Chem. Commun.*, 1986, 1504–1505.
284 P. J. Taylor, E. Kmetec and J. M. Johnson, *Anal. Chem.*, 1977, **49**, 789–794.
285 C. Figueiredo, A. García-Ortega, T. Mandal, A. Lielpetere, F. Cervantes, D. Demurtas, E. Magner, F. J. Plou, W. Schuhmann, D. Leech, M. Pita and A. L. De Lacey, *Electrochim. Acta*, 2023, **472**, 143438.
286 P. Goswami, S. S. Chinnadayyala, M. Chakraborty, A. K. Kumar and A. Kakoti, *Appl. Microbiol. Biotechnol.*, 2013, **97**, 4259–4275.
287 K. Koschorreck, S. Alpdagtas and V. B. Urlacher, *Eng. Microbiol.*, 2022, **2**, 100037.
288 Y. Mathieu, M. E. Cleveland and H. Brumer, *ACS Catal.*, 2022, **12**, 10264–10275.
289 A. Tamhankar, M. Wensien, S. A. V. Jannuzzi, S. Chatterjee, B. Lassalle-Kaiser, K. Tittmann and S. DeBeer, *J. Phys. Chem. Lett.*, 2024, **15**, 4263–4267.

 